12-2015

Validating side scan sonar as a fish survey tool

Michael A. Bollinger
The University of Texas Rio Grande Valley

VALIDATING SIDE SCAN SONAR AS A FISH SURVEY TOOL

A Thesis

by

MICHAEL A. BOLLINGER

Submitted to the Graduate College of
The University of Texas Rio Grande Valley
In partial fulfillment of the requirements for the degree of

MASTER OF SCIENCE

December 2015

Major Subject: Biology

VALIDATING SIDE SCAN SONAR AS A FISH SURVEY TOOL

A Thesis
by
MICHAEL A. BOLLINGER

COMMITTEE MEMBERS

Dr. Richard Kline
Chair of Committee

Dr. Heather Alexander
Committee Member

Dr. Carlos Cintra-Buenrostro
Committee Member

Dr. David Hicks
Committee Member

December 2015

ABSTRACT

Bollinger, Michael A., Validating Side Scan Sonar as a Fish Survey Tool. Master of Science (MS), December, 2015, 65 pp., 4 tables, 14 Figures, references, 104 titles.

Hydroacoustic methods can be used to answer a variety of questions regarding fish populations and behavior. In this study, side scan sonar methodology was developed to quantify abundance and biomass and compared to established visual observation methods on SCUBA over artificial reef structures in the western Gulf of Mexico. Side scan sonar methods were equivalent to SCUBA surveys for measuring fish abundance over the same reef areas, however, abundances were significantly higher when the larger area sampled by side scan was utilized. Side scan sonar methods were also more time efficient than SCUBA, ROV and long line fishing methods (66.7%, 33.3%, 25.9% respectively). In addition, side scan methods allowed biomass and fish size class categories to be estimated over reef sites. Side scan methods allowed five reef sites to be surveyed in one day, demonstrating the capability for macro scale comparisons of fish abundance, biomass and behavior among sites.

DEDICATION

This thesis is the compilation of two years of blood, sweat, and tears. It would not have been possible without the support of my Grandma Bubb, parents Marlin and Lynda, sister Coley, uncle Mark, cousins Steve and Chris, and my Brownsville grad student family.

ACKNOWLEDGEMENTS

I would like to thank Texas Parks and Wildlife Artificial Reef Program for funding this research. I especially need to thank my advisor and committee chair, Dr. Richard Kline, for his wild and crazy ideas, constant guidance and innumerable hours helping me shape my results and polish my writing. I'd like to acknowledge my thesis committee, Dr. David Hicks, Dr. Carlos Cintra-Buenrostro, and Dr. Heather Alexander, who have not kicked me out of their offices when I wander in with questions, and have always given encouragement and guidance. I thank Captain Andres Garcia for his patience whilst driving the towfish "around in circles". I also thank my undergraduate assistant Victor Gaytan for his help in manually counting fish backscatters and Jing Luo for his help programming in Python. I'd particularly like to acknowledge fellow graduate students Ricky Alexander and Maria Cooksey, we've been through it all together. Thank you to all of my field and lab assistants: Robert Figueroa-Downing, Gwyn Carmean, Maria Cooksey, Danny Cuevas, Catheline Froehlich, Rachel Arney, Camas Key, Liana Lerma, Jill DeMaio, Ethan Getz, Heather Otte, Shelby Bessette, Monica Delgado, Mercedes Signal-Geither. Finally I'd like to thank my family and my Brownsville grad student family for all of the support and adventures along the way.

TABLE OF CONTENTS

LIST OF TABLES

Page

LIST OF FIGURES

Page

CHAPTER I

INTRODUCTION

Hydroacoustic methods can be used to answer a variety of questions in aquatic environments (i.e. population surveys[1], long term ecological monitoring [2], behavioral surveys[3,4], etc). These methods can be used in areas that are largely inaccessible to visual census. Hydroacoustic methods, such as sonar, are becoming more prevalent as the cost of equipment decreases. Compared with early versions with printed echograms on paper, even present day consumer grade instruments are far more sophisticated. Modern day sonar equipment is being used to answer difficult questions that would otherwise be outside of the capabilities of human monitoring. These methods have been used to capture long continuous time series [2,5] or cover large areas of seafloor [6]. The large coverage area capability of hydroacoustic methods can be used to assess reef function in terms of fish use of habitat both spatially and temporally, metrics that have been a constant challenge to researchers in the past

Artificial reefs serve important functions as habitat to fishes all over the world [7]. They attract biofouling organisms such as algae, sponges and other encrusting invertebrates that provide additional structural complexity and serve as recruitment substrate [8,9]. While these reefs are generally found to increase productivity in areas that they are placed [10,11] questions remain regarding their costs and benefits and what structures provide the best outcomes over the

long-term. More assessment tools are needed to determine the types of structures and materials that are most beneficial as artificial reefs.

Reef Monitoring and Census Techniques

Reef monitoring is conducted for numerous reasons, such as determining the state of a fishery [12], the effectiveness of the reef [13], and fish behavior to better manage a fishery [14,15]. There are over 4,000 artificial reefs in the Gulf of Mexico, composed of numerous structural types, which are challenging to asses and monitor efficiently. Currently, the Texas Parks and Wildlife Department (TPWD) Artificial Reef Program (TARP) monitors 73 areas along the Texas Coast. These reefing areas typically contain multiple structures, and many additional reef deployments are planned in the future[16]. Monitoring the fish populations of these artificial reefs is an important component to both the National Artificial Reef Plan (NARP) [17] and Texas Artificial Reef Plan [16].

Current monitoring protocols for artificial reefs include: vertical long line fishing for size metrics of red snapper (*Lutjanus campechanus,* Poey, 1860), remotely operated vehicle (ROV) surveys, stationary hydroacoustic surveys and visual SCUBA surveys. While SCUBA surveys remain the most popular survey method to quantify fish abundance and biomass, they can only be performed under limited conditions [18]. ROVs can be used to survey reefs, especially when they are at depths inaccessible to SCUBA divers [15,19–21]. Visual census techniques are only useful in the range of 10s of meters in the clearest waters. In addition, the presence of a nepheloid layer (stratified layers of suspended sediments [22]) in the western Gulf makes visual surveys challenging for parts of the year [22,23]. In addition, these visual surveys provide little information regarding how reefs differ on scales larger than a diver can see or at multiple time points during a day. It is clear that management agencies need additional tools to cover larger

reefing areas with a wide variety of structural types [24]. While visual monitoring is still a major component of monitoring artificial reef deployments [16,25,26], advanced hydroacoustic methods show great potential [27–30].

Artificial Reef Fish Populations

In terms of biomass, many of the fish species commonly surveyed occur in the water column. According to quarterly visual SCUBA surveys over artificial reefs in 2014, some common species that occur in the water column were: Atlantic spadefish (*Chaetodipterus faber*, Broussonet 1782), blue runner (*Caranx crysos*, Mitchill 1815), lookdown (*Selene vomer*, Linnaeus 1758), grey triggerfish (*Balistes capriscus*, Gmelin 1789), sheepshead (*Archosargus probatocephalus*, Walbaum 1792), and the vermillion snapper (*Rhomboplites aurorubens*, Cuvier 1829). Recreationally and commercially targeted species such as red snapper (*L. campechanus*), grey snapper (*Lutjanus griseus*, Linnaeus 1758), cobia (*Rachycentron canadum,* Linnaeus 1776), and greater amberjack (*Seriola dumerili*, Risso 1810) are also commonly observed [19].

Recreational saltwater fisherman brought over $2 billion to the state of Texas in 2011 alone [31]. The majority of these economically important fishes reside in the water column - an aspect that lends itself to the use of acoustic monitoring techniques [28]. Red snapper (*L. campechanus*) is one of the most important recreationally and commercially harvested fish species [31,32] that inhabits depths from 10 m on nearshore reefs to 190 m on the shelf edge in the Gulf of Mexico [33,34]. They occur in large numbers in the water column over reefs and are important reef predators [35].

Commonly targeted fishes are regulated by size. Size classes are generally determined based on predicted ecological niches [5] or legal catch limits of economically important fishes

[36]. Categorizing reef fishes by size is a common practice used to examine the state of a fishery [36]. Knowing what genera or life stage a fish belongs to, can often help to place it in a predetermined size category. For instance, juvenile forms of all common reef fishes can be found over artificial reefs in a < 30 cm size class. Fishes comprising a 30-60 cm size class consist of red snapper, grey snapper, young amberjack, Atlantic spadefish and sheepshead. Fish species comprising a 60-90 cm size class are larger individuals of red snapper, grey snapper and amberjack. Fishes that grow larger than 90 cm are usually greater amberjack, cobia, great barracuda, African pompano (*Alectis ciliaris*, Bloch 1787) or large sharks (Scalloped Hammerhead, *Sphyrna lewini*, Griffith and Smith 1834; Bull Shark, *Carcharhinus leucas*, Müller and Henle 1839).

While it is known that large fish populations exist on artificial reefs, it is unclear what factors drive differences between reef configurations. Studies have documented fish preference for different sides of a particular reef [37] and preference for different reef configurations of the same structural type [18]. Hydroacoustic methods help to examine these factors more closely, moreover, biomass estimation of these important recreational and commercial fisheries are possible.

Fisheries Acoustics

Sonar instruments that send and receive sound waves can be used to detect fishes or objects far beyond the range of human vision and within nepheloid layers [28]. Typically, two types of data are collected from acoustic returns: time between transmission and reception, and strength of echo return. The time factor shows how far a target is away from the sound source and strength of echo return, reported as echo intensity in decibels (dB) (logarithmic ratio of an

observed to a reference intensity level) [38], can be used to show a variety of biological parameters including fish lengths [36] and community biomass estimation [39].

The wavelength (λ) of each frequency is related to the sound speed (c) and frequency (f) by $\lambda = c/f$. For each frequency, the proportion of energy reflected depends on the ratio of the λ to the size of the target [40] which is important for studies focusing on identifying microorganisms such as zooplankton [2,5,41]. For larger targets, such as fish, increased frequency enhances resolution. Fisheries acoustics generally use frequencies in the range of 10 kHz and higher [28]. The frequency chosen for a study depends on the availability of transducers and the environmental constraints of the study site. Shallow study sites (<20 m) allow for higher frequencies (>400 kHz) which generally yields higher resolution because there is smaller volume of water to attenuate the sound [40]. Conversely, deeper study sites require lower frequencies (10-200 kHz) to cover the entirety of the water column because higher frequencies would be absorbed before reaching the bottom [40], albeit with decreased resolution.

Organisms return sounds differently depending on shape, size, and body composition [41,42]. In fishes, it has long been recognized that the swim bladder is one cause of acoustic backscatter [43]. McCartney and Stubbs [44] found that backscattering cross section resolution of fish swim bladders increased with increasing frequency. However, fish with reduced swim bladder size, such as mackerel (Scombridae) or herring (Clupeidae), have an optimum frequency to yield the highest intensity [45,46]. Frequency is one way to determine acoustic fish classification [42] and target strength intensity (dB) is another [47]. Higher frequencies above ~300 kHz reveal more about the body of the fish rather than just the swimbladder. In fishes, target strength (TS) is linearly related to standard length [48], so more detailed fisheries information can be analyzed by incorporating TS.

Target Strength and Transmission Loss

Transmission strength loss from sonar can be attributed to spreading and attenuation. Spreading is defined as a geometric effect representing the regular weakening of a sound signal as it spreads outward from the source [40]. As the distance the sound has traveled increases, the area ensonified increases fourfold and the intensity decreases fourfold [49]. Attenuation, on the other hand, is the gradual loss of intensity (dB) as the sound progresses through the medium. In this case, sound intensity is lost as the wave progresses through the water. Attenuation is a function of viscosity, density, sound velocity and frequency [40]. In a shallow, well-mixed sea the only controllable variable is frequency, whereas frequency increases, absorption also increases. Spreading and attenuation become important factors and must be corrected for in post processing [50]. In many cases corrections for attenuation and spreading are done using beam angle and distance from the transducer [50].

Fisheries Acoustics Techniques

Acoustic techniques are becoming increasingly sophisticated and useful in a variety of fisheries applications. They can be used to sample large volumes of water in a short time to count acoustic echoes from fish at any depth in the water column, except right next to the seafloor and at the surface [28].

Benthic fish, such as flounder (Pleuronectidae), are indistinguishable in acoustic surveys because they are obstructed by the stronger acoustic responses of the seabed [28,38,51]. Fish that tend to aggregate over structure, rather than remaining directly on it, like snapper (Lutjanidae), jacks (Carangidae) and grouper (Epinephilininae), make appropriate targets for acoustic methods.

Abundance estimation for fish was developed in the 1950's by Tungate [52] based on the idea of simply counting individual echoes [39,51–53]. In the early 1960's investigators

developed the technology to integrate echo amplitude [53]. This integration of intensities is a standard today that is incorporated into almost all commercial and consumer grade echosounders [28].

Sonar Instruments

A variety of sonar configurations have been developed over the years for fisheries applications. A single beam echosounder is the most commonly used sonar for bottom sounding and commercial fish finders [28]. Dual beam and split beam are more specialized systems that can determine TS and return position directly from each echo [28]. Multi-beam sonar and sector scanner sonar can create radar like two-dimensional displays and can be constructed into 3D images [28,54,55]. These are widely used in creating bathymetric maps and mapping schools of fish such as herring [56]. Side scan sonar was a technology originally created to construct two-dimensional images of the seabed [28,50,57], but has been shown to be highly adaptable to other applications.

Side scan sonar was defined by Fish and Carr [58] as "an acoustic imaging device used to provide wide area, large scale pictures of the sea floor of a body of water." Side scan sonar has been used since 1963 to search for ship wrecks, look at sea floor configuration for the oil industry, and mapping benthic habitats [27,58]. The wide angle of emitted sound (beam angle) of side scan sonar allows a greater volume of water to be sampled than would be possible with a vertical echosounder [3,4,59].

Side scan units produce high quality images and side scan sonar transducers can be either attached to the hull of a vessel or mounted on a towfish (torpedo-like object tethered to a boat intended to get a transducer closer to the bottom). These units take the sonar echo and TS to create an image and these can be processed into a mosaic by merging survey lines together to

form a single image of the study site [27]. Since only one frequency is used, a wider swath of water can be covered, but less information can be retrieved from each echo return. Several studies have used side scan for observing fish including migration of salmon (Salmonidade) and herring in Canadian channels [3,4,6,59], surveying sturgeon (Acipenseridae) in the rivers of North Carolina [1,60] and counting and mapping pelagic fish schools [61]. While size classifications have occasionally been conducted with side scan sonar, no biomass estimates were noted.

Estimating Biomass

Some of the most important applications of fisheries acoustics are estimations of density, abundance, and biomass of fish [62]. An essential requirement of estimating biomass is the use of solid sphere calibration [63,64]. Two standard outputs of biomass estimation are volume backscatter strength (S_v) and TS. Volume backscatter is an integration of acoustic energy scattered from discrete targets per unit volume of water, and is often used as a proxy for fish biomass [28,62]. TS is an acoustic measurement of intensity from an individual target. Love's [48] lateral TS equation is widely used to estimate fish length from TS [65–68]. Fish length is then converted to weight using known length to weight relationships for commonly sampled fish species within the survey area [39]. Due to the lack of information regarding species identification from individual sonar returns, biomass estimates are generalizations based on the fish community sampled. Thus, it is important to know the common species that will be encountered to correctly estimate biomass [39].

Objectives and Hypotheses

The overall aim of this research was to validate side scan sonar as an additional reef survey tool. Side scan sonar units have proliferated in the marketplace from several

manufacturers with higher frequencies and convenient data recording methods. They have become popular for both recreational and commercial fishing applications and are a tool readily adapted to survey reef-associated fish [69]. A major goal of this study was to determine if side scan sonar methodology could adequately quantify fish abundance and biomass over a variety of reef structural types. To do this, fish abundance estimates using side scan sonar were compared with SCUBA surveys. The expanded coverage area of side scan sonar as compared to SCUBA was utilized to compare spatial and temporal differences in fish abundance and biomass while the costs and benefits of side scan sonar were compared to other common methodologies. The following hypothesis tested the feasibility of the side scan sonar methodology to be used as a fish census tool:

- Side scan sonar surveys will detect a higher fish abundance than SCUBA surveys within the same sites.

To analyze reef structure and the behavior of fishes over artificial reefs, two additional hypotheses were tested:

- Reef structural types will be significantly different in fish abundance and biomass as surveyed with side scan sonar.
- Fish will exhibit a preference to a side of the structure throughout the day.

CHAPTER II

METHODS

Study Sites

This study was conducted in the western Gulf of Mexico [8,18,70–72] at five representative reef structural types (Figure 1). The surface area covered for each structure was calculated from side scan sonar images using structure length and width approximated as a rectangle.

1) Culvert reef (PS-1047, N 26° 31.535', W 97° 09.215') is a nearshore TARP site of 1 km^2 area, 6.51 nm offshore of the Port Mansfield jetties, at a depth of 21 m and contains 4,922 concrete drainage culverts that are approximately 3 m in length and varying reefing density [18]. Multiple sites (see results for details) within this reef were surveyed with a mean surface area of 300 m^2. Reefed in 2011, the culvert reef represents an early successional community.

2) 3-pile jacket reef (PS-1169L, N 26° 12.902, W 96° 58.945') is a nearshore TARP site, located 7.11 nautical miles (nm) beyond the South Padre Island jetties at a depth of 24 m, containing two 3-pile oil rig jackets that are approximately 30 m long, 9 m tall. One of the 3-pile jackets has a small tugboat directly adjacent to it. The surface area of each

structure was 192 m^2. Reefed in the 1994, the 3-pile jackets are some of the latest successional states of the artificial reefs surveyed.

3) 4-pile jacket reef (PS-1070, N 26° 25.499', W 97° 01.257'), is 15.38 nm offshore from the Port Mansfield jetties. The 4-pile oil rig jackets that are 30 m long, 12 m tall and lie at a depth of 31 m. The surface area of each structure was 240 m^2. Reefed in the 1994, the 4-pile jackets represent the latest successional states of the artificial reefs surveyed.

4) Ship: The Texas Clipper Artificial Reef (PS-1122, N 26° 11.187', W 96° 51.342') lies 17.23 nm from the South Padre Island jetties and is a single, 144 m long vessel that lies 35 m depth. The surface area of this structure is 3,600 m^2. Reefed in 2007, the ship represents a middle successional state community.

*5) Natural reef (N 26° 26.127', W 97° 0.613'), Big Sea Bree reef lies at a depth of 33 m and spans 6 km. Vertical relief in this area ranges as high as 4 m. The natural reef surface area was 300 m^2 per scan. The natural reef area was assumed to be at a very late successional or climax community. *The natural reef site was used only in the rapid assessment.

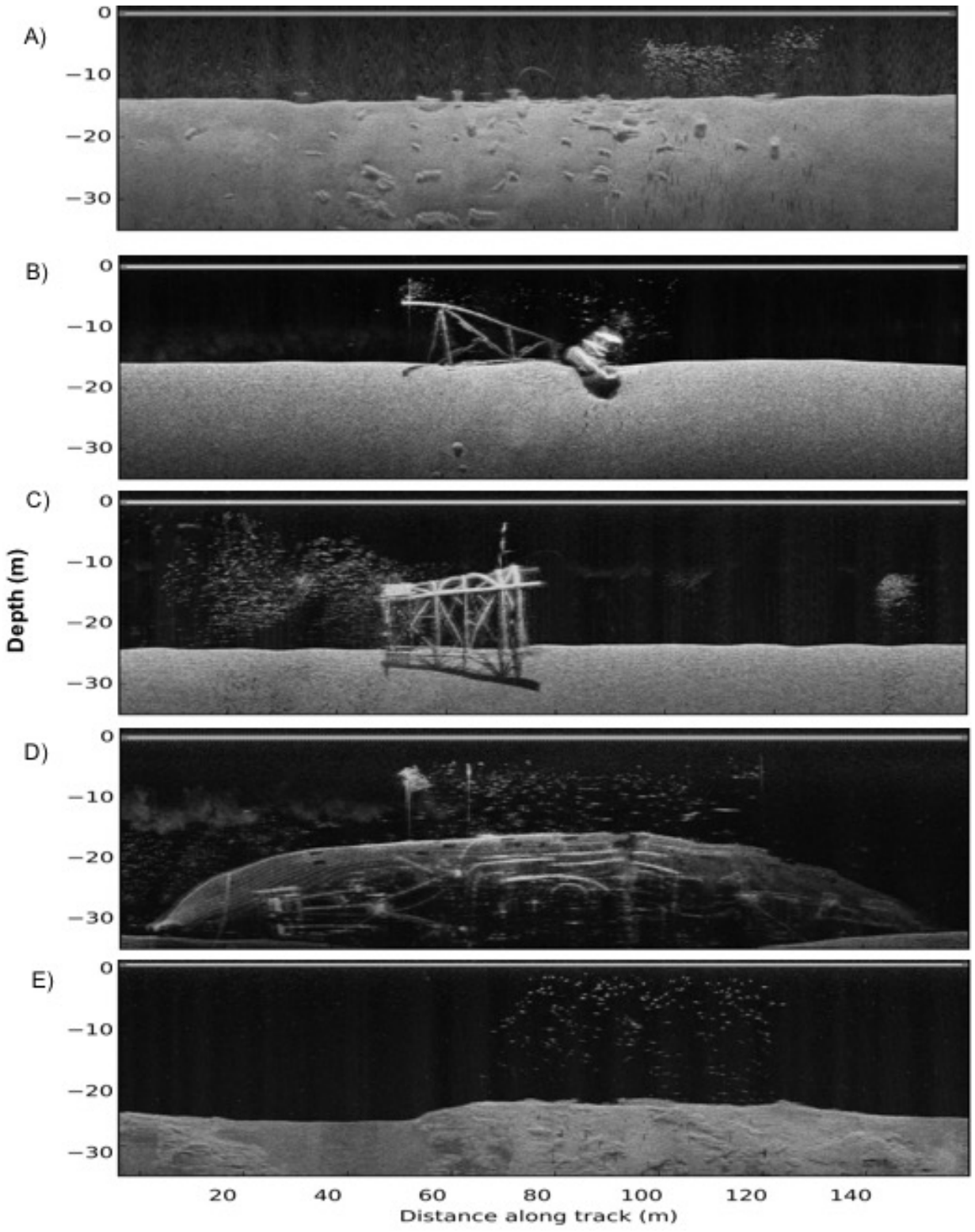

Figure 1. Side scan images of the five structural types sampled in this study. A) South Padre Island Reef, concrete culverts. B) Port Isabel Reef, 3-pile jacket. C) Port Mansfield Liberty Ship Reef, 4-pile jacket. D) Texas Clipper Reef, ship. E) Big Sea Bree, natural reef.

Sonar Equipment

A Humminbird 1198c SI Combo (Johnson Outdoors Marine Electronics, Inc., Eufaula, AL, USA) (Figure 2) was used in this study. The Humminbird has vertical beams operating at 83 kHz (60° @ -10 dB re 1 µPa) and 200 kHz (20° @ -10 dB re 1 µPa) and horizontal beams 455 kHz (86° @ -10 dB re 1 µPa; total 180° of overall coverage) and 800 kHz (55° @ -10 dB re 1 µPa; total 130° of overall coverage). The transducer (part # XPTH 14 74 HDSI T, Johnson Outdoors Marine Electronics, Inc.) was mounted in a towfish ("The Tank" part # FRO-HST, First Response Outfitters, Willis, TX, USA). The sonar equipment was further modified with waterproof connections and the transducer cable was extended (Appendix A).

Figure 2. Humminbird 1198c head unit and towfish used in this study

Range Verification

The sampling volume suggested by the manufacturer was verified using two sonar reflective Ecobuoys (Ecobouy Pty. Ltd, Malvern, Victoria, Australia) placed on a vertical line 5 m from each other and 5 m above a cement block anchor. Two identical lines were attached 5 and 10 m from the original buoy line. An additional surface marker buoy was attached at the end of the array to retrieve the buoy array and make navigation easier for the captain (Figure 3). Transects were run perpendicular to the location of the buoy array. The combined angle of the beams was verified as semicircular and measured 180°.

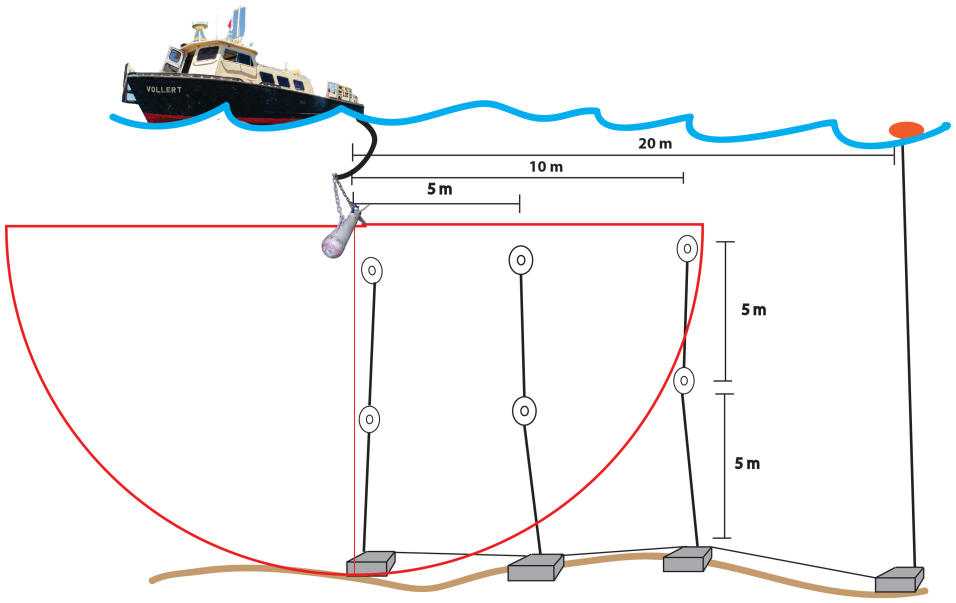

Figure 3. Schematic of the range verification experiment. Each submerged buoy was 5 m from each other and the surface marker buoy was marked with a GPS waypoint to make navigation easier.

Sonar Target Strength Calibration

Target strength (TS) of the sonar was calibrated by using solid, non-resonant, tungsten spheres of sizes 22.225 mm, 20.0 mm, 19.05 mm, 15.0 mm and 12.7 mm and a frequency of 455 kHz [63,64,73–75]. The theoretical target strength for each of the different size spheres was calculated [75], as shown in Figure 4. Equation 1 was used to calculate the backscattering cross section (σ_{BS}) of the sphere where it is related to the angular frequency (ω) in radians, the radius of the sphere (a), the sound speed in the water (c), the density of the water (ρ), the density of the sphere (ρ_1), the longitudinal wave sound speed of the sphere (c_1) and the transverse wave sound speed of the sphere (c_2).

$$\sigma_{BS} = (a^2/4)F(\omega a/c, \rho_1/\rho, c_1/c, c_2/c) \quad (1)$$

The predicted target strength of each sphere was calculated with Equation 2 [28].

$$TS = 10\mathrm{Log}_{10}(\sigma_{BS}) \quad (2)$$

The spheres were suspended in monofilament sacks attached to a 45 kg test monofilament line. Targets were passed on both the left and the right side of the transducer at distances of 5 m and 10 m.

Solid sphere calibration of the side scan sonar at 455 kHz yielded equation 3, where TS is on the y-axis and grey scale value (GSV) is on the x-axis. This equation relating GSV to TS intensity was applied to images during calibration in ImageJ.

$$TS = 0.37265(GSV) - 80.02 \quad (3)$$

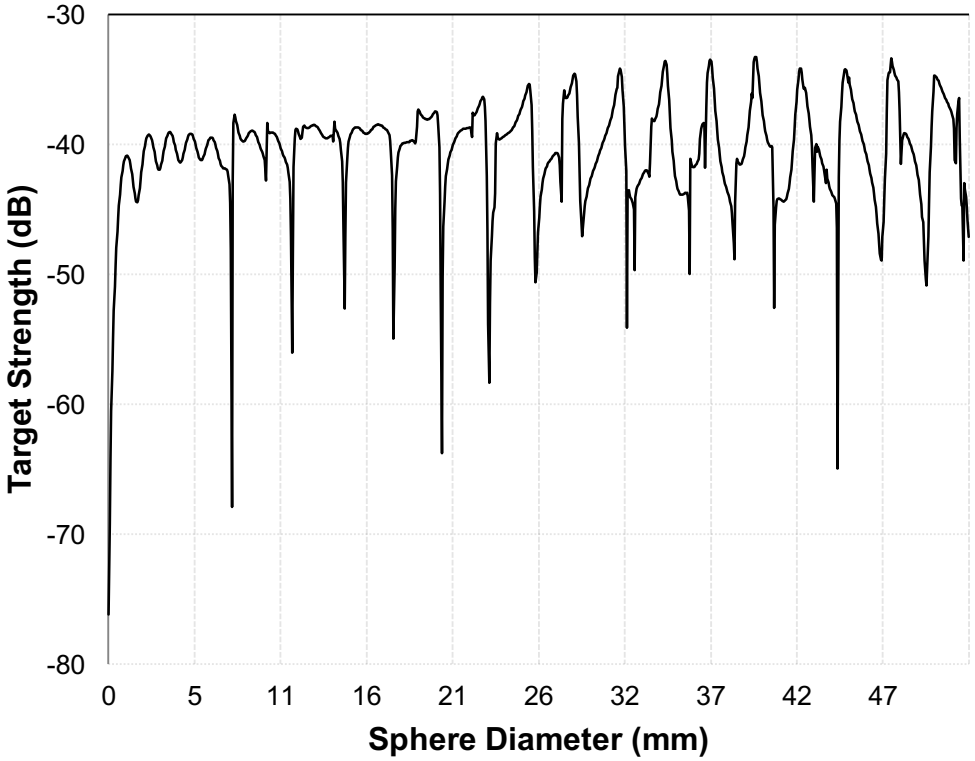

Figure 4. Theoretical target strengths for tungsten calibration spheres for 455 kHz sonars. Sharp downward peaks represent resonance within the solid sphere.

Sonar Surveys

Sonar surveys consisted of three consecutive, equal length passes over each reef structure or section of reef. After processing, only the pass with the highest abundance from each structure was used in analysis. Vessel speed was kept below 5 knots to ensure towfish was flown approximately 6 m below the surface to avoid the effects of propwash and influence of the sea surface.

SCUBA Surveys

SCUBA surveys consisted of a 15 minute modified roving diver survey [18] in which divers counted all individual fishes in the water column over the reef structure. Water column visibility (m) was recorded by divers and tested as a covariate against both sonar and SCUBA data.

Post Processing

Abundance

Images were generated with the PyHum program (v1.3.3, US Geological Survey, Flagstaff, AZ, USA [76]) written in Python (v 3.4.3, Python Software Foundation, Beaverton, OR, USA [77]). PyHum was adapted to generate water column clips from side scan sonar data (Appendix B).

Preliminary analysis of raw sonar scans revealed significant amounts of attenuation as fish target distance from the transducer increased. To correct for attenuation, a cosine-range correction was applied to the data (PyHum). Calibrated images were edited manually in Photoshop to remove bottom structure and water column interference. These images were used to calculate abundance and biomass (see next section). The processed images were opened in

ImageJ (v.1.48p, National Institutes of Health, Bethesda, MD, USA) and intensities were calibrated. Fish targets were counted and intensities recorded (Figure 5). Best fit Image J setting combinations as compared to manual counting results and image processing macro detailed in Appendices A and C, respectively.

A minimum fish TS threshold of -60 dB was determined in ImageJ and particles larger than 20 pixels and 0.05 circularity were counted. In a linear regression [78] of automated counts of fishes conducted in ImageJ vs. manual Photoshop counts, a slight underestimation of automated ImageJ counts was noted and a correction equation was applied to all sonar count data ($y = 1.1417x$; $r^2 = 0.864$; $p<0.001$; Figure 6).

Fish abundances were scaled to area of each reef structure as fish density (D_F) to make abundances more comparable among reef structure types (Equation 4).

$$D_F = \text{Total number of fish/ Reef area} \quad (4)$$

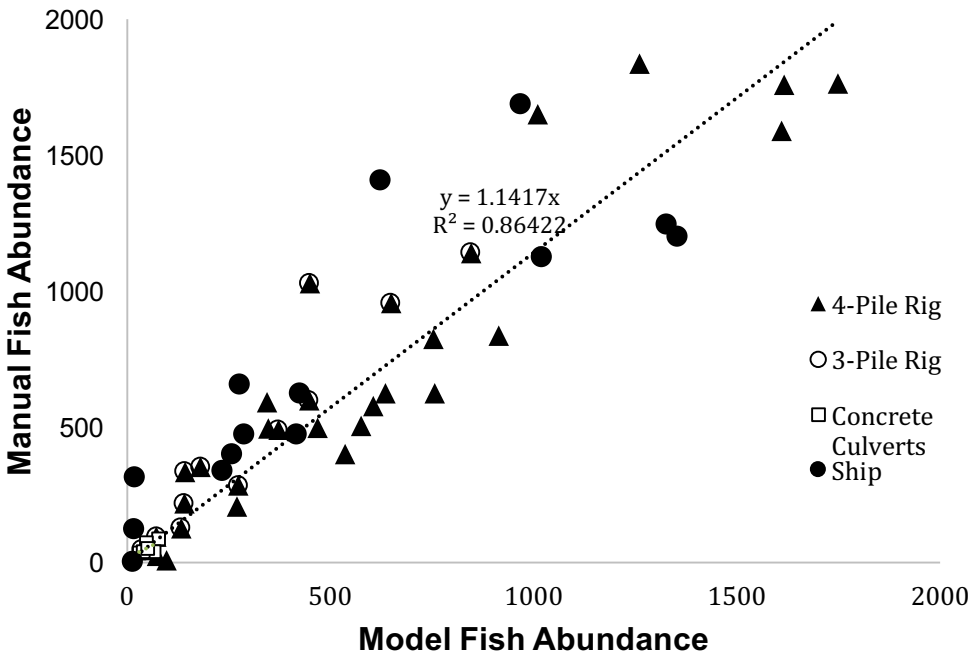

Figure 5. Manual fish counts in Photoshop compared to automated ImageJ. Linear correlation and regression were significant (R2=0.864, y=1.1417x, p<0.001). Regression equation was applied as a correction factor to the data in this study.

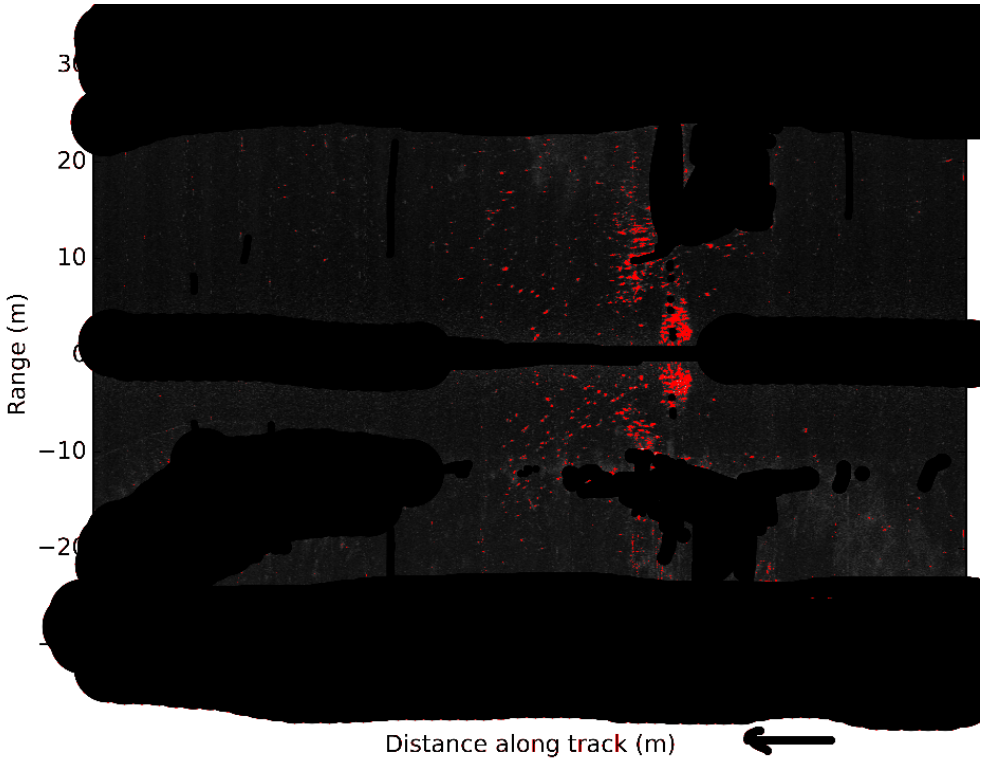

Figure 6. Example of a cleaned up image with a threshold applied in ImageJ. Fish counted manually = 340. Automated fish count = 305 * 1.1417 (correction factor) = 348.

Biomass Estimation

As detailed above, each grayscale image with the interference, seabed and reef structures removed in Photoshop was used to calculate fish TS in ImageJ. Each image was imported into ImageJ where the image was calibrated using Equation 3. Post calibration, ImageJ was used to calculate max individual TS from all targets in the image using a threshold of -60 dB, particles larger than 20 pixels, and 0.05 circularity. Fish standard length (L_{cm}) was calculated for all individuals using Equation 5 [48] and a mean standard length (cm) was determined.

$$TS = 24.1 * \log_{10}(L_{cm}) - 61 \quad (5)$$

After mean standard length was determined, a mean weight (g) was calculated using published length-to-weight relationships of commonly sampled fish species occurring over reefs in the Gulf of Mexico (see Table 1). A fish community length (L)-weight (W) relationship (Table 1, Figure 7 Equation 6) was calculated by averaging log-transformed data to form individual species growth curves.

$$W = 0.0232 * L^{2.9088} \quad (6)$$

Biomass (g/m^3) over the reefs was calculated in Equation 7 by multiplying fish density (D_F) by mean fish community weight.

$$Biomass = W * D_F \quad (7)$$

Table 1. Parameters used in calculating the mean weight to length ratio for gulf fishes, where Weight = a*(Length)b. All functions were recalculated so length was in cm and weight was in g.

Species	Max L (cm)	a	b	Source
Selene vomer	48	0.018	3.013	[79]
Lutjanus griseus	89	0.0156	2.93	[80,81]
Caranx crysos	70	0.0306	2.861	[82]
Lutjanus campechanus	100	0.01346	3.05	[83]
Balistes capriscus	60	0.03610	2.78	[81,84]
Chaetodipterus faber	91	0.03921	2.938	[85]
Archosargus probatocephalus	91	0.03415	2.89	[81,86]
Seriola dumerili	190	0.01739	2.86	[87]
Rhomboplites aurorubens	60	0.01346	3.0106	[85]

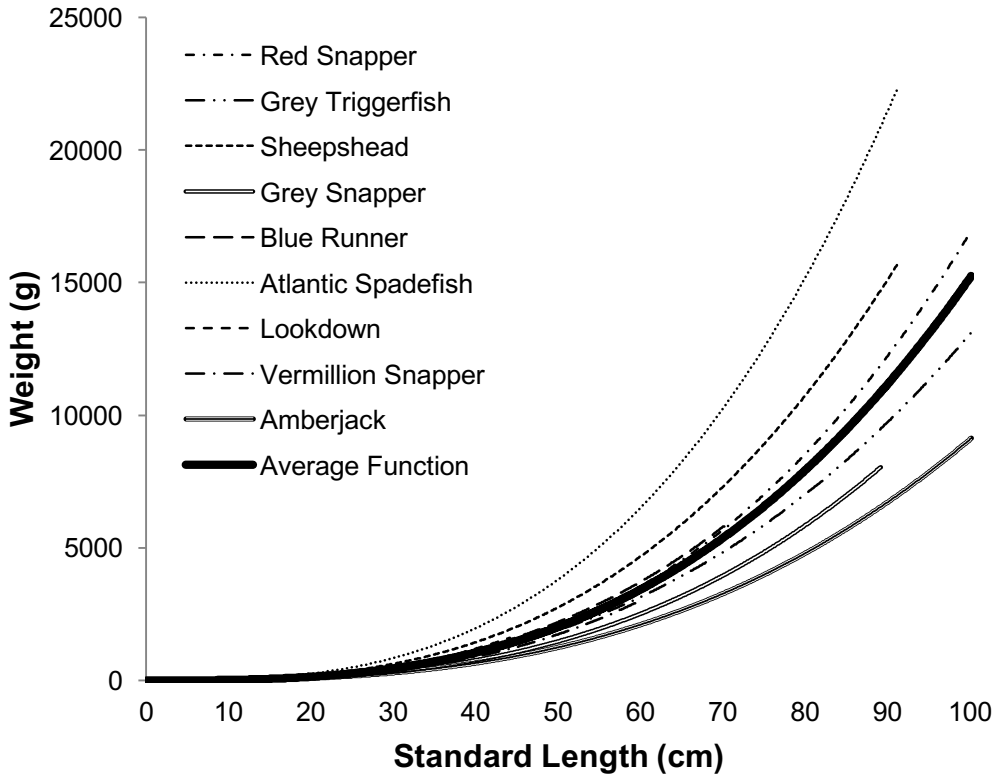

Figure 7. Weight-length ratios for common mid-water column fishes (9 total) in the Western Gulf of Mexico. The average of the ratios were calculated and plotted in bold.

Methodology Comparison

Paired side scan sonar and SCUBA counts were conducted opportunistically from May 2014 and June 2015. Visibility was noted qualitatively by divers as water column visibility (WCV) on SCUBA surveys. Water column visibility was not a significant covariate in the multivariate analysis of variance (ANOVA) comparing SCUBA and full transect sonar surveys (Sonar, $F = 0.050$, $df = 35$, $p = 0.824$; SCUBA, $F = 2.127$, $df = 35$, $p = 0.155$), therefore, paired t-tests were used in further comparisons. SCUBA abundance was compared to sonar abundance limited to the area over the structure that a diver surveyed, using a paired t-test. In addition, SCUBA abundance was compared to sonar abundance utilizing the entire transect length, with a paired t-test. All analyses were done in SPSS (v. 21 IBM Statistics, Armonk, NY, USA) unless otherwise stated.

Reef Structure Comparisons

Abundance and biomass calculated from sonar returns and scaled to each reef area was used to compare reef structures using ANOVAs with a Scheffe post hoc tests. All data was verified for normality using Q-Q plot analysis and homoscedasticity using Levine's test [78] in SPSS.

Rapid Reef Assessment

All reef comparisons were accomplished with the side scan sonar methodology detailed above. In the first comparison, four artificial reef locations and the natural reef were sampled in the same day. Three distinct sites were sampled at each location, with the exception of the ship where only one structure exists at the location. Three passes of 200 m were taken at each site where only the pass with the highest abundance was used in analysis. The reefs were compared by abundance and biomass using a multivariate ANOVA with a Scheffe post-hoc test and

verified for normality using Q-Q plot analysis and homoscedasticity using Levine's test [78] in SPSS (v. 21). Fish size classes were calculated using individual TS, determined in image J, and the Love 1969 equation. In addition, fish lengths were binned into 30 cm classes (<30cm, 30-59cm, 60-90cm, >90cm, Figure 8) as a comparison of size classes present at each reef type. Size classes were calculated as a percentage of the total fish abundance and analyzed with a Bray-Curtis similarity, multidimensional scaling plot and cluster analysis in PRIMER-E v6 package [88].

Temporal Comparison

Since preliminary surveys showed high abundances associated with 4-pile jacket structures at PS-1070, a temporal comparison was conducted to test the hypothesis that fishes exhibit a preference for a side of the structure throughout theday. Three passes of 200 m were taken at three 4-pile jacket structures during three time periods (10:00, 13:00, 18:00 hr) where only the pass from each structure and time period with the highest abundance was used in analysis. Each scan of an individual structure was divided into three sections based on cardinal direction and prevailing currents (Northwest, Southeast and over reef structure) in post processing. Repeated measures ANOVAs were used to examine abundance and biomass variation within each section of the structure with time of day and between sections of the structure with time of day. Fish size classes were also analyzed for this comparison using a multidimensional scaling plot and cluster analysis in PRIMER.

Cost and Time Efficiency

The side scan sonar methodology developed in this study to quantify reef associated fish was compared to SCUBA, remotely operated vehicle (ROV) and vertical long line fishing survey methods currently employed by TPWD. Effort in labor hours was estimated from ongoing

monitoring projects. The focus of this comparison was on time effectiveness and labor hours needed.

The cost of the Humminbird setup used in this study was compared to commercial brands of similar functioning side scan sonar (Edgetech [http://www.edgetech.com], J.W. Fishers [http://www.jwfishers.com/sss.htm], C-Max [http://www.cmaxsonar.com], Tritech [http://www.tritech.co.uk]). Pricing information was gathered from each manufacturer's website or quotes obtained from the company.

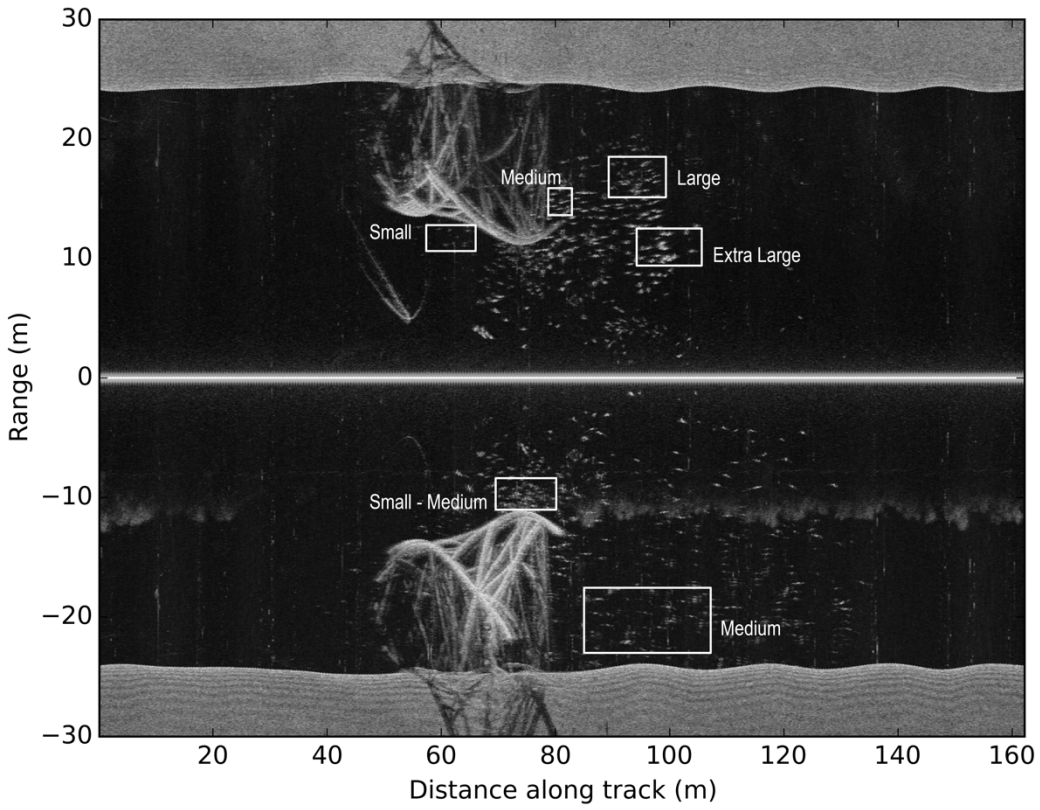

Figure 8. Example of side scan imagery with fish from each size class (small = <30cm, medium = 30-60cm, large = 60-90cm and extra large = >90cm) and a mixed size assemblage (small - medium).

CHAPTER III

RESULTS

Methodology Comparison

Counts limited to directly over the structures by side scan sonar (326.52 ± 65.65 [mean ± SE]) were not significantly different than the paired SCUBA surveys (297.25 ± 50.09) ($t = 0.259$, $df = 35$, $p = 0.797$; Figure 9A). However, side scan sonar was able to cover a much larger volume of the water than just that which is immediately around the reef structure. When considering the entire sonar recording distance (239.6 ± 72.9 m), sonar abundance (633 ± 120.91) was significantly different than the SCUBA counts ($t = -3.653$, $df = 35$, $p = 0.001$; Figure 9B).

Biomass per area reefed was significantly different among structure types ($F = 5.788$, $df = 3$, $p = 0.003$; Figure 10B). The 4-pile rig had significantly more biomass associated with it (3538.1 ± 947.7 g/m^2) than the ship (76.5 ± 21.1 g/m^2, $p = 0.048$), the culverts (453.0 ± 256.9 g/m^2, $p = 0.006$), with the 3-pile jacket being the exception (1442.9 ± 789.8 g/m^2, $p = 0.175$).

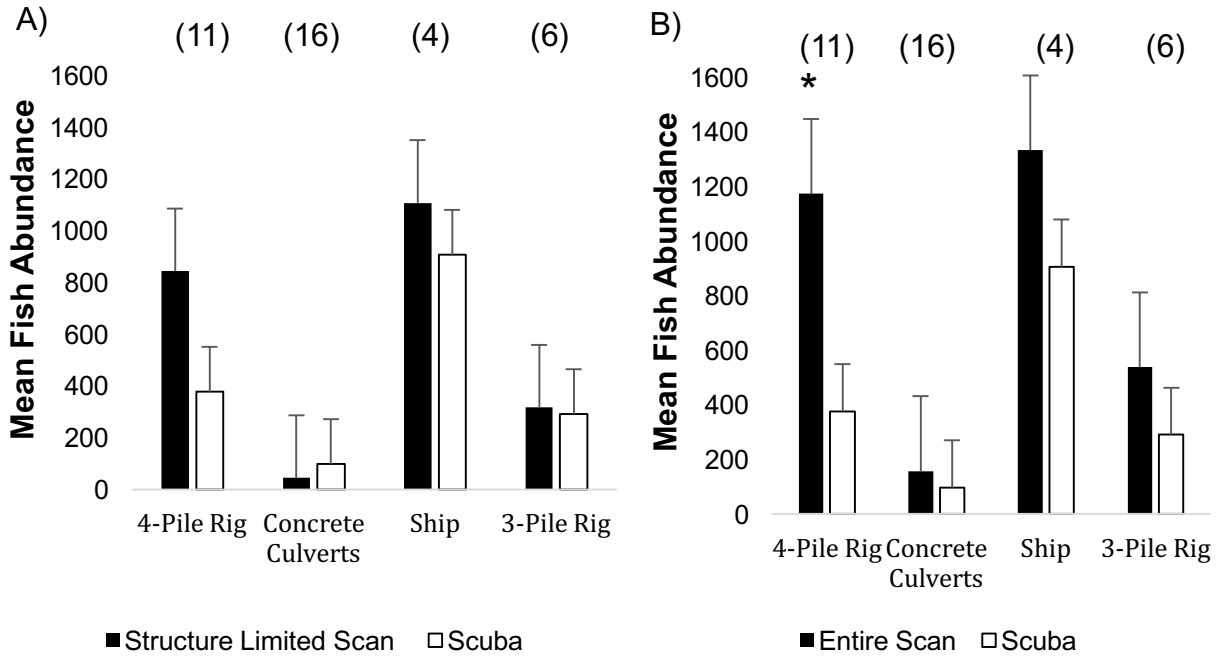

Figure 9. Sonar surveys A) limited to area over the structure (Structure Limited Scan) compared to scuba surveys of mid water column fish for each artificial reef structure ± SE (bars). B) normal length scans (Entire Scan) and compared to scuba surveys of mid water column fish for each artificial reef structure ± SE (bars). A paired T-test for limited scan and scuba were not significantly different (t=0.259, df=35, p=0.797) while a paired t-test for the entire scan and scuba was significantly different (t=-3.653, df=35, p=0.001). Further site specific paired T-tests show the 4-Pile rig is the only structure driving the significance. Sample size included in parenthesis.

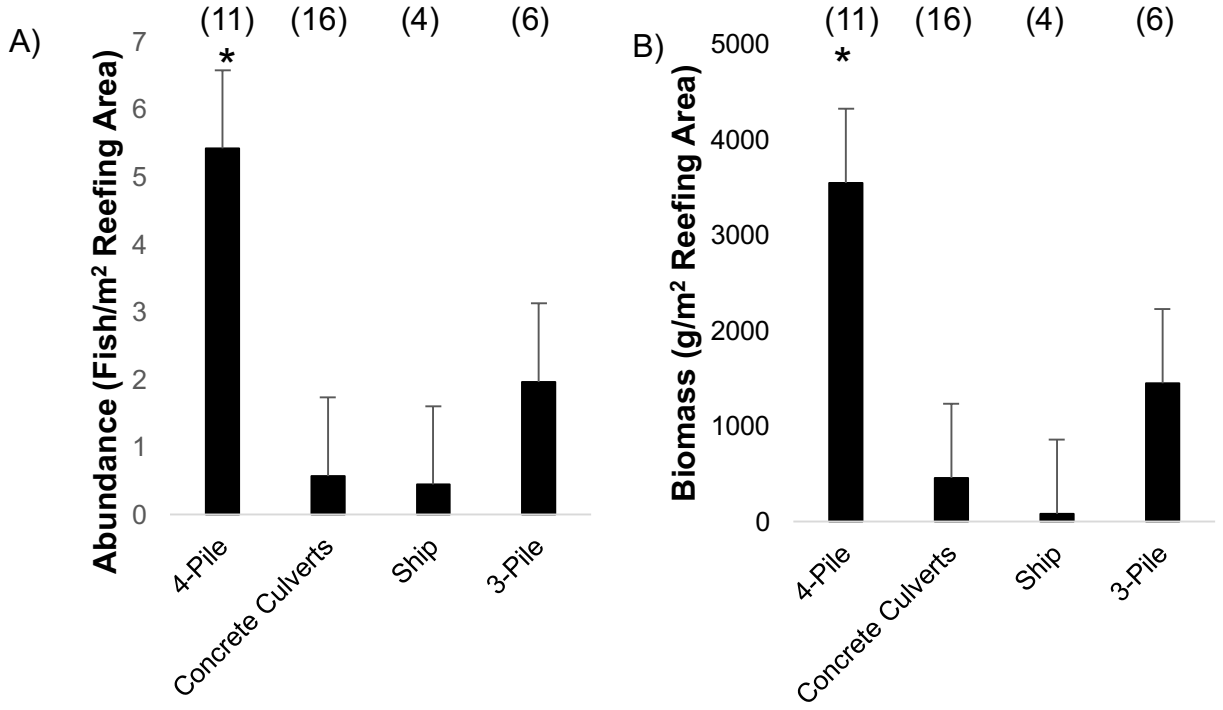

Figure 10. Abundance (A) and Biomass (B) estimates (±SE bars) per reefing area footprint for each of the artificial reef structures averaged over the study time. ANOVA (Abundance $F = 14.752$, $df = 4$, $p < 0.001$; Biomass $F = 7.200$, $df = 4$, $p < 0.001$). Sample size included in parenthesis.

Rapid Reef Assessment

An ANOVA and Scheffe post-hoc test revealed that the 4-pile jacket reef had significantly higher mean fish abundance per area reefed (4.603 ± 0.966, F = 14.752, df = 4, $p < 0.001$) than the natural site (0.154 ± 1.762 fish/m^2, $p < 0.001$), the 3-pile jackets (0.357 ± 0.406 fish/m^2, $p < 0.001$) and the culverts (0.180 ± 1.717 fish/m^2, $p < 0.001$). Ship abundances were low but were not analyzed due to low sample size (0.050 ± 1.030 fish/m^2) (Figure 11A).

In addition, the 4-pile jacket reef had significantly more biomass (5329.0 ± 1531.0 g/m^2; F = 7.200, df = 4, $p < 0.001$) associated with it than the 3-pile jacket (4.3 ± 1.2 g/m^2, p = 0.003), the culverts (137.5 ± 44.9 g/m^2, p = 0.004) and the natural site (379.6 ± 350.2 g/m^2 p = 0.007). The ship site observed low biomass but was not analyzed (26.0 ± 16.7 g/m^2) (Figure 11B).

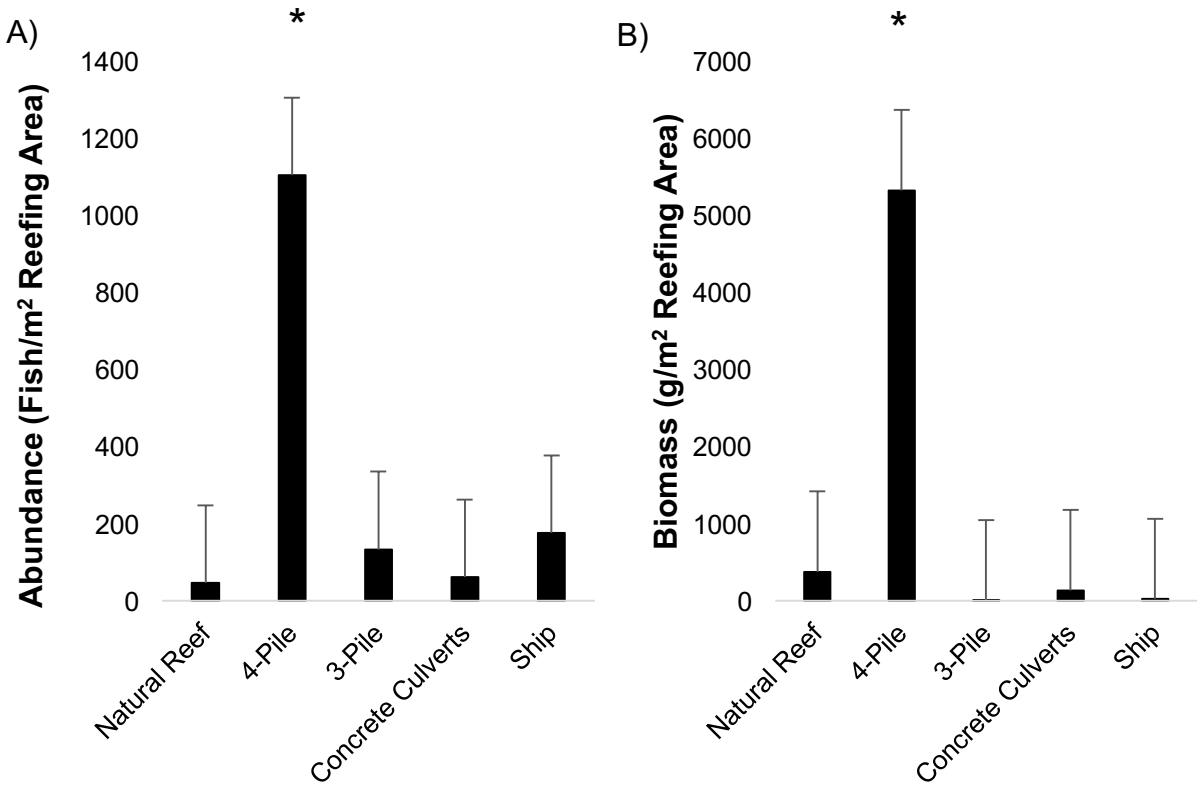

Figure 11. Abundance (A) and biomass (B) measures for each reef structure ± SE (bars) for the rapid reef assessment. A) The 4-pile jacket structures (a) are significantly greater in abundance than the other structures besides the Ship (NR p=0.001, 3-P p=0.012, CC p=0.002, Ship p=0.334). B) A similar trend is observed in biomass with higher biomass on the 4-pile rig than the other structures except for the ship (NR p=0.01, 3-P p=0.004, CC p=0.008, Ship p=0.075).

The fish assemblages by size class at concrete culvert, 4-pile jacket reefs and the ship exhibited 90% similarity to each other in the cluster analysis, while the natural reef was 80% similar. The 3-pile jacket reef was less than 60% similar to the other reef sites (Figure 12). The 3-pile jacket reef fish assemblage was smaller than other structures comprised of 1% fishes larger than 30 cm while other structures had between 45-55% of the assemblage over 30 cm (percent greater than 30 cm: natural 55.2%, 4-pile 46.8%, culverts 45.1%, ship 43.4%; Figure 12).

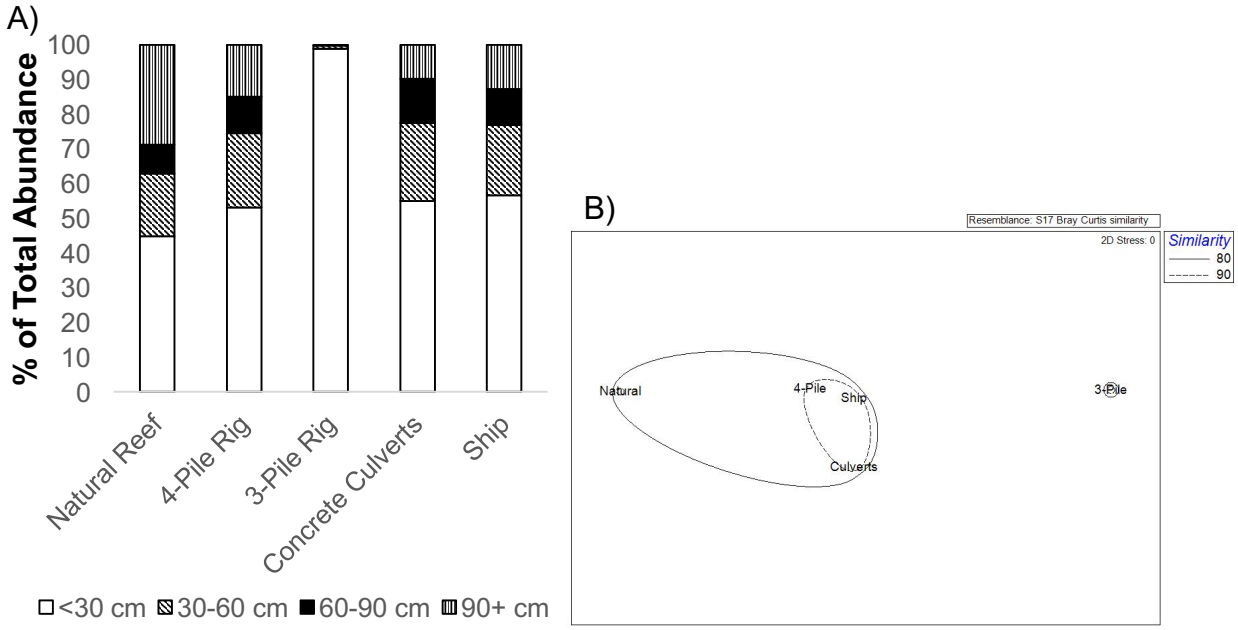

Figure 12. A) Fishes size class abundances for each reef structure scaled to 100 percent of the total abundance. B) Multidimensional scaling plot of fishes size classes at each reef location with 80 and 90% similarity groupings. The 4-Pile, Ship and Concrete Culverts are >90% similar to each other and the natural reef is within 80% similarity to the aforementioned three.

Temporal Comparison

The comparison of the 4-pile jacket reef structures over an eight-hour period showed a decrease in the abundance of reef fishes directly over the structure as the day went on (Repeated measures ANOVA, within; over $F = 31.034$, $df = 2$, $p = 0.001$; Figure 13A). While no significant change in fish abundances was noted on the NW and SE ends of the structure throughout the day (NW, $F = 0.654$, $p = 0.450$; SE, $F = 0.05$, $p = 0.948$). Total abundance showed a decreasing trend

that was not significant regardless of position over the structure ($F = 0.639$, $df = 2$, $p = 0.531$; means: AM 0.758 ± 0.082, Noon 0.711 ± 0.105, PM 0.471 ± 0.043).

A similar decreasing trend with time period was observed with biomass. Biomass over the structure decreased as the day progressed and biomass on the northwest side hit a minimum during the midday sampling, although not significantly (Repeated measures ANOVA within; over $F = 3.280$, $df = 2$, $p = 0.073$; NW $F = 0.369$, $p = 0.699$; SE $F = 0.014$, $p = 0.979$; Figure 13B). No significant differences were observed within sections of the reef. Size classes showed high similarity (>80%) between the jacket structures and time of day (Figure 14). Each of the structures showed a drop in larger fish above 30 cm as the day progressed (Platform 1: AM 39.0%, Noon 20.5%, PM 31.9%; Platform 2: AM 49.2%, Noon 39.0%, PM 19.6%; Platform 3: AM 43.6%, Noon 45.0%, PM 24.3%).

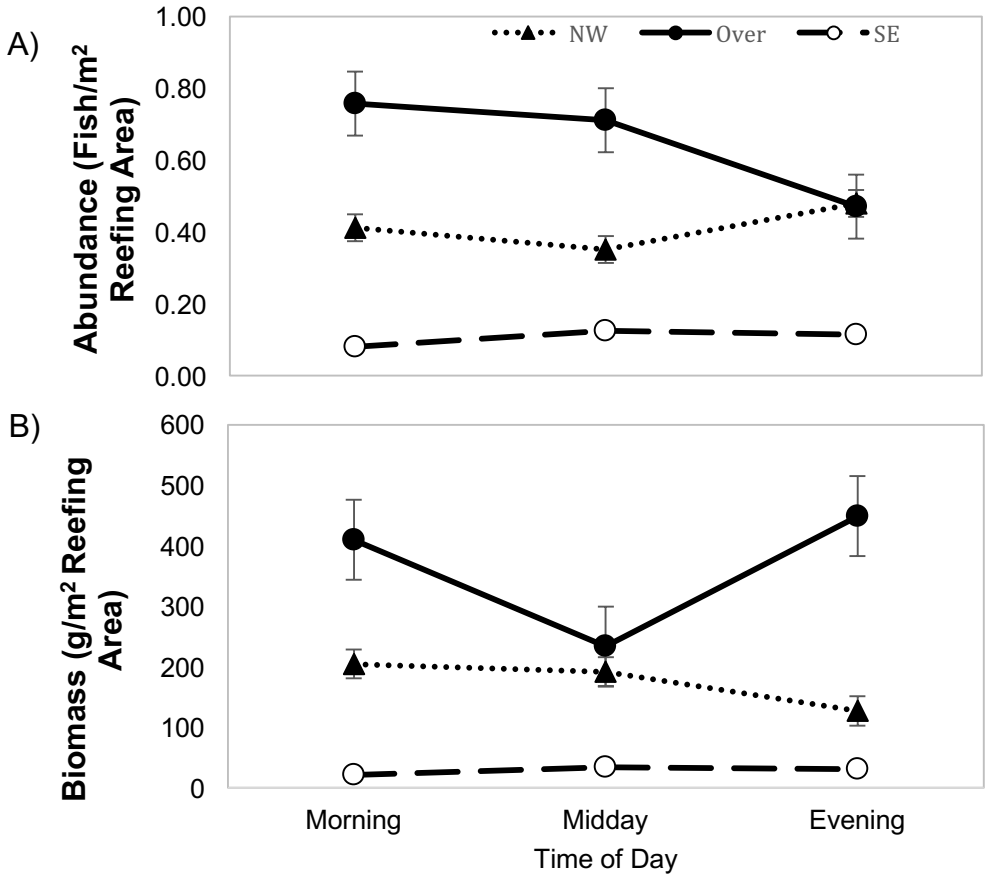

Figure 13. Abundance (A) and biomass (B) estimates on the SE side, NW side and over the top of 4-pile jacket structures, at the Port Mansfield Liberty Ship Reef (PS-1070) ± SE (bars). The over structure abundance decreased during a daily sampling regime (Repeated Measures ANOVA, F=31.034, df=2, p=0.001) while biomass seemed to diminish during the midday samples (Repeated Measures ANOVA, F=6.500, df=2, p=0.012). Fishes abundance and biomass ahead and behind of the structure (with respect to currents) did not change significantly.

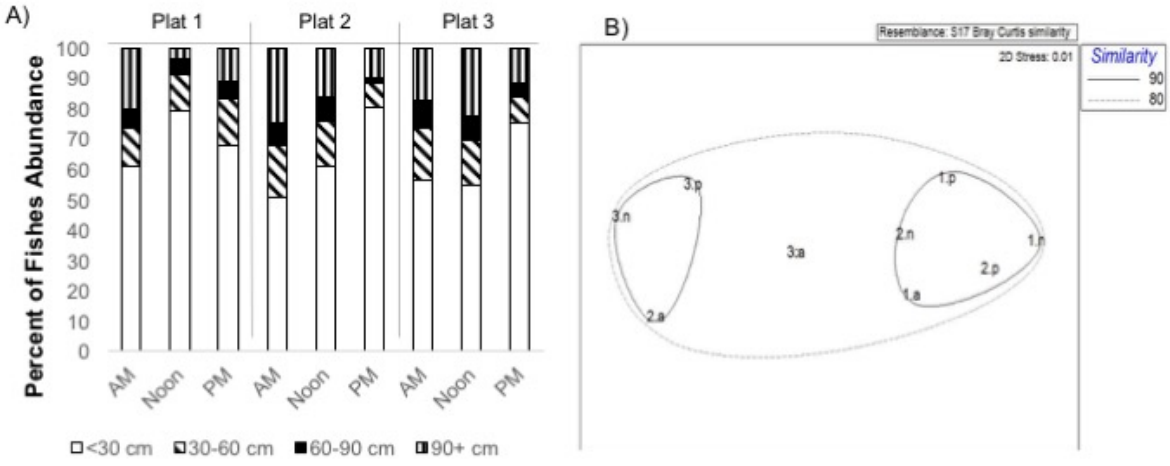

Figure 14. A) Fishes size class abundances for each platform (plat) structure and time scaled to 100 percent of the total abundance. B) Multidimensional scaling plot of fish size classes at each platform structure and time (Plat Number.Time) with 80 and 90% similarity groupings. All structures and times are greater than 80% similar.

Cost Benefit Analysis

The time effectiveness comparison showed that for surveys of four sites, using the methodologies defined in this study, side scan sonar used a total of 40 labor hours which included data collection and processing time (Table 2). Side scan sonar took approximately 25.9% less time than vertical long line fishing, and 66.7% less time than SCUBA surveys to cover the same areas.

The cost analysis showed that the Humminbird configuration in this study was 35.9% less expensive than the least expensive commercial unit (Table 3). The prices ranged from $7,800 to $40,000. In addition, all others required a user-supplied computer to record the data that was not in the estimates.

Table 2. Time efficiency calculation for side scan sonar, remotely operated vehicle, long line fishing and scuba surveys as outlined by TPWD SOP and approximate time needed to complete surveys at Padre South Artificial Reef Sites. Man Hours = Man Power ((4/ Sites per day)*(Travel Time) + (Time at Site * 4)) + Processing Time

	Man power	Time at Site (hr)	Sites/day	Travel time/ day	Total Field Time (4 sites)	Processing time	Labor Hours
SS	2	0.5	4	6	8	24	40
ROV	2	1	4	6	10	40	60
Fishing	2	3	1	3.25	25	4	54
Scuba	4	4	1	3.25	29	4	120

Table 3. Cost effectiveness of the Humminbird system used in this study including all necessary software and modification hardware compared to published costs of other packages.

System Used in this Study		Other Packages	
Sonar	$2,300	Edgetech	$35,000
Towfish	$1,000	J.W.Fishers	$25,000
Hardware	$600	C-Max	$40,000
Software	$1,100	Tritech 990F	$7,800
Total	$5,000		

CHAPTER IV

DISCUSSION

Abundance, biomass and size categories of reef fish were calculated with the use of a low cost and efficient method of processing side scan sonar data. To the author's knowledge, this is the first study to use side scan sonar for the quantification of reef fish abundance and biomass. Abundance estimates of reef fish using the side scan sonar method proved to be comparable to SCUBA surveys, when restricted to the same coverage area, indicating its utility in reef surveys. Multiple studies ground truth their sonar surveys with trawl net tows [89] which would prove difficult on any reef structure. A main advantage of sonar is that it is not limited to the area directly over the structure in SCUBA surveys. The temporal comparison showed high fish abundance on end of the structure, possibly indicating a behavioral preference. Demonstrating that reef fish aggregations cannot be quantified using the SCUBA survey method in some cases.

The sonar methodology quantified more fish than SCUBA when extending the survey into a larger water volume. A few studies have taken advantage of this large-scale water column sampling technique [6,90] and have been successful in enumerating fishes. Trevarrow [90] was able to count migrating salmon using a stationary side scan sonar but was unable to determine TS. Other studies have used a split beam or dual-beam echo sounder [28,89,91,92] but side scan's fanlike beam pattern allow it to ensonify a larger water volume in a single pass [90]. One drawback of active acoustic methods and a reason SCUBA surveys cannot be completely

replaced by sonar, is a lack of clear species differentiation. Species identification is thought of as the “grand challenge of fisheries and plankton acoustics” [68] and some recent studies have shown promise [93–95].

Although species identification was not accomplished, the present study categorized reef fish into 30 cm increments for effective reef comparison. Jordan [96] showed a similar categorization of reef fishes in visual studies where fish lengths were broken down into five categories to look at small scale changes on artificial patch reefs. The present study was able to categorize fishes by length based on calibrated target strength, which is similar to other acoustic surveys where species identification has not been achieved [36,42]. Walline [36] was able to differentiate between three acoustically determined size classes of pelagic fish using Simrad single-beam sonar where their size classes were based on commercial catches. Similarly, the present study chose size classes that are based on the minimum recreational limits for commonly observed species.

Habitat Comparisons

In this study, the 4-pile jacket structures had significantly higher abundances surrounding them than any of the other structure types (Figure 11). Oil platform jacket structures have been reported to hold high abundance and diversity of fishes in other studies [19,97]. However, location may also play a role in the higher abundance observed. Garcia [71] suggested inshore sites, like the culvert reef, are fished more because of their location in state managed waters than offshore locations, like the ship, because of their location in federally managed waters. The 4-pile structures were farther offshore and may have had reduced fishing pressure due to the lack of a surface marker buoy and extended closures of the U.S. federal fishing seasons for red snapper and amberjack. The 4-pile jackets have been reefed the longest and should represent the

latest successional community surveyed which could account for some of the high fish abundances observed.

In the rapid assessment, the 3-pile jacket structures closer to shore had the lowest abundances despite their structural and reefing age similarities to the 4-pile jackets. Fishing pressure might have played a role in the differences observed at the 3-pile jacket structures due to their proximity to South Padre Island and the US-Mexican border. While fishing pressure and reef structure type are two obvious factors that may be associated with the observed differences in fishes, other parameters such as proximity to the coast, depth, currents as well as biological parameters (e.g., recruitment rates of biofouling which will support the trophic web, competition for resources, predation pressure) could account for variation in the differences observed and further studies are warranted.

The size class differences observed at the 3-pile jacket in this study also support that fishing pressure may be the cause of the differences observed. The 3-pile jacket sites showed no fish above 60 cm during the reef comparison analysis, which may indicate predator depletion, likely from fishing [98]. Other sites showed a more even distribution of size classes especially above 60 cm and likely representative of predators. However, the biomass estimates for the overall method comparisons suggested a presence of higher numbers of fishes and larger individuals that were not observed in the single day reef comparison study. This may indicate a seasonal component and more reef comparison surveys are needed to draw further conclusions.

The temporal comparison showed clear differences in fish abundances on different sides of the structures (Figure 13). Boswell et al. [24] showed fish abundance decreased as distance from the reef complex increased. Decreasing fish abundance with distance away from the structure was noted in most cases during the present study, fishes were consistently more

numerous on one end of the structure than the other. A potential reason for this side preference could be feeding patterns of the planktivorous species. Hamner et al. [37] found planktivorous fishes on the great barrier reef form a “wall of mouths” on the upstream, side of the reef where larger fishes would be farther from and smaller fishes would be closer to the reef.

Fishes abundance at the structures tended to decrease as the day progressed (Figure 13). It is also well documented that fishes show diel feeding patterns [99,100]. This result shows the importance of timing any survey to be able to accurately sample the entire population. A feature easy to accomplish with side scan sonar but very difficult to accomplish with any visual methods.

Boswell et al. [39] reported methodology for determining biomass in g/m^3 of water volume sampled, and Boswell et al. [24] showed acoustic biomass in volume backscatter (S_v). This study scaled biomasses to reef surface area to account for reef size differences and make the structures comparable. Both are acceptable methods for reporting the statistic [28]. Boswell et al. [24], covered an entire artificial reef, but made no comparisons of other structures as conducted in this study. In the present study, fishes were assumed to be associated with the reef structure so these scaled results could be used to make inferences regarding each of the reef structures.

Low Cost High Efficiency

The cost-benefit analysis showed that side scan sonar is a low cost, high efficiency method for quantification of reef fish. The rapid assessment of reef structures with side scan sonar demonstrated in this study would allow managers to sample multiple sites in a single day which creates a large data set of comparable data. Large datasets are now manageable with the accessibility of large storage devices and faster processors [101,102]. The ability to collect large amounts of acoustic data over a numerous structural types can be advantageous because multiple questions can be answered from a single data set.

The use of the Hummingbird and SD memory card recording made the data acquisition convenient and economical. The present method used the programs HumViewer, PyHum and ImageJ, all freeware, coupled with Adobe Photoshop to create a semi-automated method to process the side scan sonar data. Many commercial sonar packages require expensive software and annual service agreements in addition to the purchase of the hardware. Boswell [103] outlined methodology to partially automate processing of dual-frequency identification sonar (DIDSON) data. Automating the data processing streamlined the method and cut down the labor needed to obtain results using this method. Freeware, such as PyHum, cuts down on the initial cost of starting a project and because it is based on an open source program, it can be highly adaptable. In another study, Buscombe [50] used a Humminbird sidescan sonar and PyHum to classify sediments on a riverbed. The adaptability of side scan sonar and the convenience of the Humminbird platform allow new uses to be discovered without large start-up costs.

Future Applications

The reef comparisons in this study show how the side scan methodology can answer macro-scale questions about artificial reefs. However, questions that can be answered using the methodology are not limited to artificial reefs or macro-scale analyses. This methodology can be adapted for a number of different aquatic environments. A lower frequency or increasing tow-cable length would allow sampling in deeper habitats. Conversely, using the methodology in shallower habitats, like a lake [104], can be accomplished by using a shorter cable or a hull mounted transducer. The adaptability and affordability of side scan sonar will make it an attractive option for fisheries managers all over the world. The side scan methodology reported here allows large scale comparisons of numerous reef habitats for reef fish abundance, size classes and biomass in a variety of sea states and visibility levels.

REFERENCES

1. Flowers HJ, Hightower JE. Estimating Sturgeon Abundance in the Carolinas Using Side-Scan Sonar. Mar Coast Fish. 2015;7: 1–9. doi:10.1080/19425120.2014.982334

2. Miksis-Olds JL, Stabeno PJ, Napp JM, Pinchuk AI, Nystuen JA, Warren JD, et al. Ecosystem response to a temporary sea ice retreat in the Bering Sea: Winter 2009. Prog Oceanogr. 2013;111: 38–51. doi:10.1016/j.pocean.2012.10.010

3. Trevorrow MV, Pedersen B. Detection of migratory herring in a shallow channel using 12- and 100-kHz sidescan sonars. Aquat Living Resour. 2000;13: 395–401.

4. Trevorrow MV. Detection of migrating salmon in the Fraser River using 100-kHz sidescan sonars. Can J Fish Aquat Sci. 1997;54: 1619–1629.

5. Miksis-Olds JL, Stauffer SA. Understanding the relationship between ice, primary producers, and consumers in the Bering Sea. J Acoust Soc Am. 2014;136: 2186–2186.

6. Trevorrow MV, Claytor RR. Detection of Atlantic herring (Clupea harengus) schools in shallow waters using high-frequency sidescan sonars. Can J Fish Aquat Sci. 1998;55: 1419–1429.

7. Brickhill MJ, Lee SY, Connolly RM. Fishes associated with artificial reefs: attributing changes to attraction or production using novel approaches. J Fish Biol. 2005;67: 53–71.

8. Arney RN. Recruitment patterns of juvenile fish at an artificial reef in the Gulf of Mexico [Internet]. 2014. Available: http://repositories.tdl.org/utb-ir/handle/2152.6/555

9. Stone RB, Pratt HL, Parker Jr RO, Davis GE. A comparison of fish populations on an artificial and natural reef in the Florida Keys [Internet]. National Marine Fisheries Service; 1979. Available: http://spo.nmfs.noaa.gov/mfr419/mfr4191.pdf

10. Bohnsack JA. Are high densities of fishes at artificial reefs the result of habitat limitation or behavioral preference? Bull Mar Sci. 1989;44: 631–645.

11. Stone RB. National Artificial Reef Plan. NOAA Tech Memo NMFS -6 US Dep Commer Wash DC. 1985; 70.

12. SEDAR. SEDAR 31 - Gulf of Mexico Red Snapper Stock Assesment Report. Southeast Data, Assessment and Review; 2013.

13. Alevizon WS, Gorham JC. Effects of artificial reef deployment on nearby resident fishes. Bull Mar Sci. 1989;44: 646–661.

14. Santos M. Diurnal variations in the fish assemblage at an artificial reef. ICES J Mar Sci. 2002;59: S32–S35. doi:10.1006/jmsc.2001.1166

15. Stoner AW, Ryer CH, Parker SJ, Auster PJ, Wakefield WW. Evaluating the role of fish behavior in surveys conducted with underwater vehicles. Can J Fish Aquat Sci. 2008;65: 1230–1243. doi:10.1139/F08-032

16. Stephan CD, Dansby B, Osburn H, Matlock G, Riechers R, Rayburn R. Texas Artificial Reef Fishery Management Plan. Texas Parks and Wildlife Department; 2013.

17. NARP. National Artificial Reef Plan (as Ammended):guidelines for siting, construction, development and assesment of artificial reefs. 2007.

18. Froehlich CYM, Kline RJ. Using Fish Population Metrics to Compare the Effects of Artificial Reef Density. Layman CA, editor. PLOS ONE. 2015;10: e0139444. doi:10.1371/journal.pone.0139444

19. Ajemian MJ, Wetz JJ, Shipley-Lozano B, Shively JD, Stunz GW. An Analysis of Artificial Reef Fish Community Structure along the Northwestern Gulf of Mexico Shelf: Potential Impacts of "Rigs-to-Reefs" Programs. Layman CA, editor. PLOS ONE. 2015;10: e0126354. doi:10.1371/journal.pone.0126354

20. Kraus RT, Hill RL, Rooker JR, Dellapenna TM. Preliminary characterization of a mid-shelf bank in the northwestern Gulf of Mexico as essential habitat of reef fishes. 2006. pp. 621–632. Available: http://procs.gcfi.org/pdf/gcfi_57-43.pdf

21. McIntyre FD, Collie N, Stewart M, Scala L, Fernandes PG. A visual survey technique for deep-water fishes: estimating anglerfish *Lophius* spp. abundance in closed areas [a]: a visual survey method for *lophius* spp. J Fish Biol. 2013; n/a–n/a. doi:10.1111/jfb.12114

22. Shideler GL. Development of the benthic nepheloid layer on the South Texas continental shelf, Western Gulf of Mexico. Mar Geol. 1981;41: 37–61. doi:10.1016/0025-3227(81)90103-1

23. McGrail DW, Carnes M. Shelfedge dynamics and the nepheloid layer in the northwestern Gulf of Mexico. Soc Econ Paleontol Mineral. 1983; 251–263.

24. Boswell KM, Wells RJD, Cowan, Jr. JH, Wilson CA. Biomass, Density, and Size Distributions of Fishes Associated with a Large-Scale Artificial Reef Complex in the Gulf of Mexico. Bull Mar Sci. 2010;86: 879–889. doi:10.5343/bms.2010.1026

25. Baine M. Artificial reefs: a review of their design, application, management and performance. Ocean Coast Manag. 2001;44: 241–259.

26. Bohnsack JA, Sutherland DL. Artificial reef research: a review with recommendations for future priorities. Bull Mar Sci. 1985;37: 11–39.

27. Cuevas KJ, Buchanan MV, Moss D. Utilizing side scan sonar as an artificial reef management tool. IEEE; 2002. pp. 136–140. Available: http://ieeexplore.ieee.org/xpls/abs_all.jsp?arnumber=1193260

28. Simmonds J, MacLennan D. Fisheries Acoustics: Theory and Practice. 2nd ed. Blackwell Science Ltd.; 2005.

29. Stanley DR, Wilson CA. Abundance of fishes associated with a petroleum platform as measured with dual-beam hydroacoustics. ICES J Mar Sci J Cons. 1996;53: 473–475.

30. Stanley DR, Wilson CA. Variation in the density and species composition of fishes associated with three petroleum platforms using dual beam hydroacoustics. Fish Res. 2000;47: 161–172.

31. ASA sportfishing in America report. American Sportfishing Association; 2013.

32. Gillig D, Griffin WL, Ozuna T. A Bioeconomic Assessment of Gulf of Mexico Red Snapper Management Policies. Trans Am Fish Soc. 2001;130: 117–129. doi:10.1577/1548-8659(2001)130<0117:ABAOGO>2.0.CO;2

33. Gallaway BJ, Szedlmayer ST, Gazey WJ. A life history review for red snapper in the Gulf of Mexico with an evaluation of the importance of offshore petroleum platforms and other artificial reefs. Rev Fish Sci. 2009;17: 48–67. doi:10.1080/10641260802160717

34. Allen GR. Snappers of the world: an annotated and illustrated catalogue of Lutjanid species known to date. Rome: Food and Agriculture Organization of the United Nations; 1985.

35. Wells R, Cowan J, Fry B. Feeding ecology of red snapper Lutjanus campechanus in the northern Gulf of Mexico. Mar Ecol Prog Ser. 2008;361: 213–225. doi:10.3354/meps07425

36. Walline PD, Pisanty S, Lindem T. Acoustic assessment of the number of pelagic fish in Lake Kinneret, Israel. Hydrobiologia. 1992;231: 153–163.

37. Hamner WM, Jones MS, Carleton JH, Hauri IR, Williams DM. Zooplankton, planktivorous fish, and water currents on a windward reef face: Great Barrier Reef, Australia. Bull Mar Sci. 1988;42: 459–479.

38. Horne JK. Acoustic approaches to remote species identification: a review. Fish Oceanogr. 2000;9: 356–371.

39. Boswell KM, Wilson MP, Wilson CA. Hydroacoustics as a tool for assessing fish biomass and size distribution associated with discrete shallow water estuarine habitats in Louisiana. Estuaries Coasts. 2007;30: 607–617.

40. Urick RJ. Principals of Underwater Sound. 3rd ed. Los Altos, CA: Peninsula Publishing; 1983.

41. Warren JD, Stanton TK, McGehee DE, Chu D. Effect of animal orientation on acoustic estimates of zooplankton properties. Ocean Eng IEEE J Of. 2002;27: 130–138.

42. Borstad GA, Lemon DD, Martinez M. Monitoring of zooplankton vertical distribution and abundance with acoustic water column profilers. 2009; Available: http://citeseerx.ist.psu.edu/viewdoc/download?doi=10.1.1.158.5179&rep=rep1&type=pdf

43. Cushing DH, Richardson ID. Echo sounding experiments on fish. 1955.

44. McCartney BS, Stubbs AR. Measurements of the acoustic target strengths of fish in dorsal aspect, including swimbladder resonance. J Sound Vib. 1971;15: 397–420. doi:10.1016/0022-460X(71)90433-0

45. Edwards JI, Armstrong F, Magurran AE, Pitcher TJ. Herring, mackerel and sprat target strength experiments with behavioural observations. ICES CM. 1984;1984: 1–31.

46. Degnbol P, Lassen H, Staehr KJ. In-situ determination of target strength of herring and sprat at 38 and 120 kHz. Dana. 1985;5: 45–54.

47. MacLennan DN. Acoustical measurement of fish abundance. J Acoust Soc Am. 1990;87: 1–15.

48. Love RH. Maximum Side-Aspect Target Strength of an Individual Fish. J Acoust Soc Am. 1969;46: 746–752.

49. Bradley D, Stern R. Underwater Sound and the Marine Mammal Acoustic Environment: A Guide to Fundamental Principals. US Mar Mammal Comm. 2008;

50. Buscombe D, Grams PE, Smith SM. Automated riverbed sediment classification using low-cost sidescan sonar. J Hydraul Eng. 2015; 06015019.

51. Misund OA. Underwater acoustics in marine fisheries and fisheries research. Rev Fish Biol Fish. 1997;7: 1–34.

52. Tungate DS. Echo-sounder surveys in the Autumn of 1956: Fishery investigations. H.M. Stationary Office; 1958.

53. Mitson RB, Wood R j. An automatic method of counting fish echos. J Cons Int Explor Mer. 1962;26: 281–291.

54. Gerlotto F, Soria M, Fréon P. From two dimensions to three: the use of multibeam sonar for a new approach in fisheries acoustics. Can J Fish Aquat Sci. 1999;56: 6–12.

55. Gerlotto F, Fréon P, Soria M, Cottais PH, Ronzier L. Exhaustive observation of 3D school structure using multibeam side scan sonar: potential use for school classification, biomass estimation and behaviour studies. ICES CM. 1994;1994: B–26.

56. Misund OA, Aglen A, Hamre J, Ona E, Røttingen I, Skagen D, et al. Improved mapping of schooling fish near the surface: comparison of abundance estimates obtained by sonar and echo integration. ICES J Mar Sci J Cons. 1996;53: 383–388.

57. Grace R, Kerr V, Conservancy N. Intertidal and subtidal habitats of Doubtless Bay, Northland, NZ. 2005; Available:

http://www.marinenz.org.nz/documents/Grace_and_Kerr_2005_Doubtless_Bay_Report-no_maps.pdf

58. Fish JP, Carr HA. Sound underwater images: a guide to the generation and interpretation of side scan sonar data. Lower Cape Pub.; 1990.

59. Trevorrow MV. Salmon and herring school detection in shallow waters using sidescan sonars. Fish Res. 1998;35: 5–14.

60. Flowers HJ, Hightower JE. A Novel Approach to Surveying Sturgeon Using Side-Scan Sonar and Occupancy Modeling. Mar Coast Fish. 2013;5: 211–223. doi:10.1080/19425120.2013.816396

61. Smith PE. The horizontal dimensions and abundance of fish schools in the upper mixed layer as measured by sonar. Proceedings of an international symposium on biological sound scattering in the ocean. 1970.

62. Maclennan D. A consistent approach to definitions and symbols in fisheries acoustics. ICES J Mar Sci. 2002;59: 365–369. doi:10.1006/jmsc.2001.1158

63. Foote KG. Spheres for calibrating an eleven-frequency acoustic measurement system. J Cons ICES J Mar Sci. 1990;46: 284–286.

64. MacLennan DN. The Theory of Solid Spheres as Sonar Calibration Targets. Department of Agriculture and Fisheries for Scotland; 1981.

65. Boswell KM, Kaller MD, Cowan JH, Wilson CA. Evaluation of target strength–fish length equation choices for estimating estuarine fish biomass. Hydrobiologia. 2008;610: 113–123. doi:10.1007/s10750-008-9425-x

66. Love RH. Target strength of an individual fish at any aspect. J Acoust Soc Am. 1977;62.

67. Foote KG. Fish target strengths for use in echo integrator surveys. Jounal Acoust Soc Am. 1987;82: 981–987.

68. MacLennan DN, Holliday DV. Fisheries and plankton acoustics: past, present and future. ICES J Mar Sci. 1996;53: 513–516.

69. Daniels M, Frank D, Holloway R, Kowalski B, Krone-Davis P. Evaluating Good Water Quality Habitat for Steelhead in Carmel Lagoon. 2009; Available: http://ccows.csumb.edu/pubs/reports/CSUMB_ENVS660_ClassReport_CarmelLagoon_100618d_fw.pdf

70. Froehlich CY. A comparison of fish communities over different reef configurations in the northwestern Gulf of Mexico [Internet]. 2014. Available: http://repositories.tdl.org/utb-ir/handle/2152.6/618

71. Garcia A. A comparison of site fidelity and habitat use of red snapper (*Lutjanus campechanus*) to evaluate the performance of two artificial reefs in South Texas utilizing acoustic telemetry [Internet]. 2013. Available: http://repositories.tdl.org/utb-ir/handle/2152.2/458

72. Alexander R. Comparing reproductive capacities of nearshore and offshore red snapper, Lutjanus campechanus, on artificial reefs in the Western Gulf of Mexico. University of Texas Rio Grande Valley. 2015.

73. Faran J. Sound scattering by solid cylinders and spheres. Jounal Acoust Soc Am. 1951;23: 405–418.

74. Hickling R. Analysis of echoes from a solid elastic sphere in water. Jounal Acoust Soc Am. 1962;34: 1582–1592.

75. MacLennan DN. Target strength measurements on metal spheres [Internet]. Librarian Department of Agriculture and Fisheries for Scotland, Marine Laboratory; 1982. Available: http://134.19.161.249/Uploads/Documents/SFRR25.pdf

76. Buscombe D, Hamill D. PyHum [Internet]. United States Geological Survey; 2015. Available: https://github.com/dbuscombe-usgs/PyHum

77. van Rossum G. Python [Internet]. Beaverton, OR, USA: Python Software Froundation; 2001. Available: www.python.org

78. Sokal RR, Rohlf FJ. Biometry: the principles andpractice of statistics in biological research. WH Freeman Co San Franc SokalBiometry Princ Pract Stat Biol Res. 1995;

79. Oliveira Freitas M, Machado Vasconcelos S, Hostim-Silva M, Spach HL. Length-weight relationships for fishes caught by shrimp trawl in Santa Catarina coast, south Atlantic, Brazil. J Appl Ichthyol. 2011;27: 1427–1428. doi:10.1111/j.1439-0426.2011.01749.x

80. Powers SP, Grabowski JH, Peterson CH, Lindberg WJ. Estimating enhancement of fish production by offshore artificial reefs: uncertainty exhibited by divergent scenarios. Mar Ecol Prog Ser. 2003;264: 265–277.

81. South Atlantic Fishery Management Council. Fishery management plan, regulatory impact review, and final environmental impact statement for the snapper-grouper fishery of the south Atlantic region. NMFS, Charelston, SC; 1983.

82. Frota LO, Costa PAS, Braga AC. Length-weight relationships of marine fishes from the central Brazilian coast. NAGA WorldFish Cent Q. 2004;27: 20–26.

83. McInerny SA. Age and growth of red snapper, Lutjanus campechanus, from the southeastern United States [Internet]. University of North Carolina. 2007. Available: http://www.sefsc.noaa.gov/sedar/download/SEDAR24-RD02_McInerny2007.pdf?id=DOCUMENT

84. Ismen A, Muhammet T, Yigin CC. The Age, Growth and Reproduction of Gray Triggerfish (Balistes capriscus, Gemelin, 1789) in Iskenderun Bay. Pak J Biol Sci. 2004;7: 2135–2138.

85. Wigley SE, McBride HM, McHugh NJ. Length-Weight Relationships for 74 Fish Species Collected during NEFSC Research Vessel Bottom Trawl Surveys, 1992-99. National Marine Fisheries Service; 2003.

86. Dutka-Gianelli J, Murie DJ. Age and growth of sheepshead, Archosargus probatocephalus (Pisces: Sparidae), from the northwest coast of Florida. Bull Mar Sci. 2001;68: 69–83.

87. Manooch III CS, Potts JC. Age, growth, and mortality of greater amberjack, Seriola dumerili, from the US Gulf of Mexico headboat fishery. Bull Mar Sci. 1997;61: 671–683.

88. Clarke K, Gorley R. PRIMER v6: User Manual/Tutorial. Plymouth, U.K.: PRIMER-E; 2006.

89. Misund OA. Underwater acoustics in marine fisheries and fisheries research. Rev Fish Biol Fish. 1997;7: 1–34.

90. Trevorrow MV. Detection of migrating salmon in the Fraser River using 100-kHz sidescan sonars. Can J Fish Aquat Sci. 1997;54: 1619–1629.

91. Stanley DR, Wilson CA. Abundance of fishes associated with a petroleum platform as measured with dual-beam hydroacoustics. ICES J Mar Sci J Cons. 1996;53: 473–475.

92. Stanley DR, Wilson CA. Effect of scuba divers on fish density and target strength estimates from stationary dual-beam hydroacoustics. Trans Am Fish Soc. 1995;124: 946–949.

93. Lawson G. Species identification of pelagic fish schools on the South African continental shelf using acoustic descriptors and ancillary information. ICES J Mar Sci. 2001;58: 275–287. doi:10.1006/jmsc.2000.1009

94. LeFeuvre P, Rose GA, Gosine R, Hale R, Pearson W, Khan R. Acoustic species identification in the Northwest Atlantic using digital image processing. Fish Res. 2000;47: 137–147.

95. Korneliussen RJ, Heggelund Y, Eliassen IK, Johansen GO. Acoustic species identification of schooling fish. ICES J Mar Sci J Cons. 2009;66: 1111–1118.

96. Jordan LKB, Gilliam DS, Spieler RE. Reef fish assemblage structure affected by small-scale spacing and size variations of artificial patch reefs. J Exp Mar Biol Ecol. 2005;326: 170–186. doi:10.1016/j.jembe.2005.05.023

97. Ajemian MJ, Wetz JJ, Shipley-Lozano B, Stunz GW. Rapid assessment of fish communities on submerged oil and gas platform reefs using remotely operated vehicles. Fish Res. 2015;167: 143–155. doi:10.1016/j.fishres.2015.02.011

98. Jennings S, Polunin NVC. Impacts of predator depletion by fishing on the biomass and diversity of non-target reef fish communities. Coral Reefs. 1997;16: 71–82.

99. Helfman GS. Fish behaviour by day, night and twilight. The behaviour of teleost fishes. Springer; 1986. pp. 366–387.

100. Ouzts AC, Szedlmayer ST. Diel Feeding Patterns of Red Snapper on Artificial Reefs in the North-Central Gulf of Mexico. Trans Am Fish Soc. 2003;132: 1186–1193. doi:10.1577/T02-085

101. Zhang J, Huang K, Cottman-Fields M, Truskinger A, Roe P, Duan S, et al. Managing and Analysing Big Audio Data for Environmental Monitoring. IEEE; 2013. pp. 997–1004. doi:10.1109/CSE.2013.146

102. Truskinger A, Cottman-Fields M, Eichinski P, Towsey M, Roe P. Practical Analysis of Big Acoustic Sensor Data for Environmental Monitoring. IEEE; 2014. pp. 91–98. doi:10.1109/BDCloud.2014.29

103. Boswell KM, Wilson MP, Cowan JH. A semiautomated approach to estimating fish size, abundance, and behavior from dual-frequency identification sonar (DIDSON) data. North Am J Fish Manag. 2008;28: 799–807. doi:10.1577/M07-116.1

104. Fleischer GW, Argyle RL, Curtis GL. In situ relations of target strength to fish size for Great Lakes pelagic planktivores. Trans Am Fish Soc. 1997;126: 786–794.

APPENDIX A

APPENDIX A

MODIFICATIONS AND DETAILED SIDE SCAN SONAR METHODOLOGY

Humminbird Settings

The "transducer" selection was set to the hi-def sidescan. "Side Imaging Frequency" was set to 455 kHz. Only this side imaging frequency was used to maximize resolution of fishes backscatter, while taking into account transmission loss due to attenuation. The side scan "Range" was set to 30 m past the known maximum depth of each site to accurately sample the whole water volume. "SI Sensitivity" was set at 15 and "Chart Speed" at 10. "Down Imaging" was set to 200 kHz. "Water Type" was set to Salt. All other defaults were followed in the unit.

Modifications

The following modifications to the standard Humminbird and towfish were made: (1) the transducer cable was extended using a 60 m cat-7 data cable (part # Hyperline-SSTP4-C7 Certicable, Farmington, NY, USA) to bear the load of the towfish as it is pulled through the water; (2) a connector (part # MCIL8, SubConn Inc., MacArtney Underwater Technology Group, Esbjerg, Denmark) was added between the towfish and the cable extension to ease the storage of both the cable and the towfish; (3) each of the connections were wrapped in aluminum mylar tape (Marine Tech Wire and Cable Inc., York, PA, USA) to prevent interference between wires; (4) the head unit's power cable was adapted to fit a small 12v battery with an inline fuse, to adapt

to a wide range of vessels on which this set up can be used; (5) a longer cable was fitted for the units GPS transmitter; (6) to solidify the headunit-transducer connection a Lowrance™ transducer extension cable (part # XT-10BLK, Lowrance Electronics, Tulsa, OK, USA) was used to connect the circuit board inside the head unit to the transducer; (7) the towfish was hot-dip galvanized to protect the metal from the marine environment.

As the Humminbird head unit ages, the connectors on the back panel become fatigued and cease to make reliable connections. Occasionally the power cable would become unconnected and the devise would shut off, or the GPS cable would become unplugged and all sonar data collected was unusable. For these reasons, the connectors on the back panel were replaced with higher quality screw link connectors. A Lowrance™ transducer extension cable (part# XT-10BLK, Lowrance Electronics, Tulsa, OK, USA) was used for the transducer connection and two 4-pin connectors (part# 43-00092, 43-00100 Conec Corp., Garner, NC, USA) were used for the power and GPS connections.

Sampling Notes

When collecting data, shortening the towfish cable length pulled the towfish up into the water column enough so that bubbles entrained from the vessel propellers were visible in the scans. This is a source of interference that was corrected by slowing the towing speed of the vessel or lengthening the towfish cable. Electrical interference was induced when pumps drawing high currents were activated. This was mitigated by connecting the sonar directly to the boat's 12v power supply and a small 12v UPC battery as a buffer to prevent surges.

Python Method

To run the adapted PyHum code (Appendix B) one must section the original recording in HumViewer (v.86) using the Utilities>Create Sub Recording tool. All *.dat and associated folders to be analyzed must be able to be located in the same file directory. The user has to put the file directory and shortcut name in the associated "filepathWin.txt" or "filepathMac.txt" depending on the operating system. The program will also prompt users to input a crop depth into the terminal to isolate the water column in the images.

Preliminary analysis of raw sonar scans revealed significant amounts of attenuation as fishes distance from the transducer increased. To get accurate biomass estimates, the PyHum image correction module was employed. The module scales scan data into dB W (Watts) where it uses a cosine-range correction to find the incident angle of the pings. The incident angle coupled with the height above the seabed were used to calculate the ping intensities scaled to distance away from the transducer.

SonarTRX Method

Side scan sonar recordings can also be processed using SonarTRX (v.15.1, Leraand Engineering Inc., Honolulu, HI, USA) for a license fee. The original recording was processed in SonarTRX to determine average depth and distance of the recording. Additionally, each recording was sectioned using the clip feature in the "View and Edit" tab. Clips were made so that the structure or point being sampled was centered in the middle of the clip. The clips were started after a boat turn was completed and before the next turn was started. Creating clips allows you to process all of the images from the original recording at once.

The manual abundance count images were further processed under the Create Mosaic tab where master images were created without slant range correcting (SRC) the data, the highest resolution, color scheme “Spectrum HV-2D”, “Auto” image correction, Force heading “90”, and the range was cropped on all channels to a meter more than the average depth (e.g. Depth=30, cropped at “31”). These settings created a master image containing all the tiles from the both sonar sides. The master image (.tiff) is then opened in Photoshop (CS6 v.13.0.1, Adobe Inc.) where backscatters on the image are counted using the counting tool (under the eyedropper tool).

For the automated particle count, the settings were slightly different in SonarTRX. Under the Create Mosaic tab where master images were created without SRC, the highest resolution, color scheme “Grey values”, “None” image correction, Force heading “90”, and the range was cropped on all channels to a meter more than the average depth (e.g. Depth=30, cropped at “31”). Grayscale master images were then imported into Photoshop where any interference, reef structure and the bottom was removed using the eraser tool. This same image will be used in the biomass methodology in the image J processing section.

Image J Processing

Images were calibrated, counted and had intensities recorded in ImageJ. Macros were written to streamline and loop processing (Appendix C). Images were first set to 8-bit grey scale using Images > Type > 8-bit. Then calibrated using Equation 8 in Analyze>Calibrate where a straight line and grey scale need to be selected. Using the determined calibration equation, the x and y data can be populated with values that lie on the calibration line. Calibration equations will have to be determined for each devise and frequency used using the solid sphere methodology detailed above. A threshold was set using Image >Adjust >Threshold Settings>Set (e.g., Lower: -

55 (dB); Upper: -10 (dB)), then particles were counted using Analyze>Analyze Particles (e.g. Size: “60-Infinity”, Circularity: 0.15-1) (Table 4).

Table 4. Parameters referenced in Image J counting model. See text for details.

Structure	Lower Threshold	Pixel Size Selection	Circularity Lower Limit
Sonar TRX (Ship)	-60	60	0.10
Sonar TRX (Rig)	-55	70	0.10
Sonar TRX (Low Relief)	-51	70	0.15
PyHum	-60	20	0.05

To retrieve individual scatterer TS (i.e. fish size classification) the results from each image analysis must be saved. The macro saves this automatically, but to do it manually, process the image like normal. When the “results” dialog opens, find File> Save As and make sure to change the file extenton to the desired output (i.e. *.xls, *.csv, etc.). From the spredsheet use the Love equation to transform the TS to fish length.

APPENDIX B

APPENDIX B

PYHUM CODE

Filename: “filepathWin.txt”

It is important that the nickname is in all caps and all of the file paths line up.

NICKNAME	File path
BONSAI	C:\\Users\\Student\\Documents\\Mike\\Side_Scan_Data\\Reef_Comparison\\Bonsai
ABUNDANCE	C:\\Users\\Student\\Documents\\Mike\\Side_Scan_Data\\Abundance
FISHING	C:\\Users\\Student\\Documents\\Mike\\Side_Scan_Data\\Fishing_Experiment

Filename: “filepathMac.txt”

Mac users can use this file path dictionary. Insert your own filepath and nickname for the folder that your .dat files occupy.

NICKNAME	File path
BONSAI	C:\\Users\\Student\\Documents\\Mike\\Side_Scan_Data\\Reef_Comparison\\Bonsai
DAILY	C:\\Users\\Student\\Documents\\Mike\\Side_Scan_Data\\Reef_Comparison\\Daily_Comparison
ABUNDANCE	C:\\Users\\Student\\Documents\\Mike\\Side_Scan_Data\\Abundance

For instructions on installing PyHum visit https://github.com/dbuscombe-usgs/PyHum. It is nessesary to install all suggested libraries along with the PyHum module. After install, running the following python code, in terminal, will process Humminbird data exactly as processed in this study. It is important to keep the “filepathWin” or “filepathMac” in the same folder as the following code. You can find this code on https://github.com/MBollinger89/PyHumAdaptation.

```
#!/usr/bin/python
import PyHum

import numpy as np

import matplotlib.pyplot as plt

import os

from scipy.io import loadmat

import sys

import sonar_file_path as sfp
import platform

#=================================================
# Read sonar data. Do it first
def read_sondata(hmf,sonDir,c1,f1,model1,chunk1):
    PyHum.read(hmf,sonDir,c=c1,f=f1,model=model1,chunk=chunk1)


#=================================================
# correct scans
def correct(humfiles,sonpath,cww):
    PyHum.correct(humfiles,sonpath,correct_withwater=cww)


#=================================================
# Define a function to put chunks together and crop by depth
def custom_save(figdirec,root):
    # Save the figure

plt.savefig(os.path.normpath(os.path.join(figdirec,root)),bbox_inches='tig
ht',dpi=800)

#=================================================


def process(humfile,sonpath,depth):
    # Process the chunks and crop

    # if son path name supplied has no separator at end, put one on
    maxy = depth
    print 'Crop size '+str(maxy)+' meters'
    if sonpath[-1]!=os.sep:
        sonpath = sonpath + os.sep


    base = humfile.split('.DAT') # get base of file name for output

    base = base[0].split(os.sep)[-1]
```

```
    # remove underscores, negatives and spaces from basename

    if base.find('_')>-1:

        base = base[:base.find('_')]

    if base.find('-')>-1:

        base = base[:base.find('-')]

    if base.find(' ')>-1:

     base = base[:base.find(' ')]

    if base.find('.')>-1:
        base = base[:base.find('.')]



    #load metadata file in

    meta =
loadmat(os.path.normpath(os.path.join(sonpath,base+'meta.mat')))

    shape_port = np.squeeze(meta['shape_port'])
    shape_star = np.squeeze(meta['shape_star'])

    with
open(os.path.normpath(os.path.join(sonpath,base+'_data_port_lw.dat')),
'r') as ff:
        port_fpw = np.memmap(ff, dtype='float32', mode='r',
shape=tuple(shape_port))

    with
open(os.path.normpath(os.path.join(sonpath,base+'_data_star_lw.dat')),
'r') as ff:
        star_fpw = np.memmap(ff, dtype='float32', mode='r',
shape=tuple(shape_star))

    Zdist = meta['dist_m']
    extent = shape_port[0]
    ft = np.squeeze(1/meta['pix_m'])

    fig = plt.figure()
    plt.imshow(np.vstack((np.flipud(port_fpw), star_fpw)), cmap='gray',
extent=[np.min(Zdist), np.max(Zdist), -extent*(1/ft), extent*(1/ft)])
    plt.ylabel('Range (m)'), plt.xlabel('Distance along track (m)')

    plt.axis('normal'); plt.axis('tight')
    plt.ylim(-maxy, maxy)

    imagepath = os.path.basename(humfile)
    imagename = os.path.splitext(imagepath)[0]
```

```
plt.savefig(os.path.normpath(os.path.join(sonpath,imagename+'.png')),bbox_
inches='tight',dpi=800)
    del fig


    print 'image name =', imagename



if __name__=="__main__":

    if len(sys.argv)==1:
        dataName = raw_input("please put your data set name\n")
        depth = raw_input("please put the depth of the water in meters\n")
        #dist = raw_input ("please put the distance of the scan in
meteres\n")

    elif len(sys.argv)==2 and sys.argv[1].isdigit():
        distFlag = raw_input("Is this the distance of your scan?
(yes/no)")

        #if distFlag.upper()=='YES' or distFlag.upper()=='Y':
        #    depth = raw_input("please put the depth of the water in
meters\n")
        #    dist = sys.argv[1]

        #elif distFlag.upper()=='NO' or distFlag.upper()=='N':
        #    #dist = raw_input ("please put the distance of the scan in
meteres\n")
        #    depth = sys.argv[1]

        dir=raw_input("please put your directory path\n")


    elif  len(sys.argv)==2 and not sys.argv[1].isdigit():
        depth = raw_input("please put the depth of the water in meters\n")
        #dist = raw_input ("please put the distance of the scan in
meteres\n")
        dir = sys.argv[1]

    else:
        #dist = sys.argv[3]

        depth = sys.argv[2]

        dir = sys.argv[1]

    depth = float(depth)
    if platform.system()=='Windows':
        pathfile = 'filepathWin.txt'
    elif platform.system()=='Darwin':
```

```
        pathfile = 'filepathMac.txt'
    else:
        raise OSError('Unknown operating system')

    dir = sfp.find_path(dataName,pathfile)
    humfiles = [each for each in os.listdir(dir) if each.endswith('.DAT')]
    if not dir[-2:]==os.sep:
        dir=dir+os.sep

    humfiles = [dir+fname for fname in humfiles]

    sonDir = [filename[:-4] for filename in humfiles ]

    #Read Parameters
    c1 = 1560 # speed of sound Salt water (m/s)
    f1 = 455 # frequency kHz of sidescan sonar
    model1 = 1198 # humminbird model
    chunk1 = 1


    # Correct Parameters
    cww = 1 #correct with water; 0=No water, 1=water


    testFlag = raw_input("Is this a testing run?(yes/no)")

    #For Single File test.....
    if testFlag.upper()=='YES' or testFlag.upper()=='Y':
        print "Runing test for file "+humfiles[0]
        mat = [each for each in os.listdir(sonDir[0]) if
each.endswith('.mat')]
        if mat ==[]:
            print "Read data first!"
            print "Reading....."
            read_sondata(humfiles[0],sonDir[0],c1,f1,model1,chunk1)
            print "Finish reading"

        print "Correcting : "+humfiles[0]
        correct(humfiles[0],sonDir[0],cww)
        print "Finished Correcting"

        print "Processing : "+humfiles[0]
        process(humfiles[0],sonDir[0],depth)

    elif testFlag.upper()=='NO' or testFlag.upper()=='N':
        #For all files in directory, use.....
        for humf,sonD in zip(humfiles,sonDir):
            print "Start Process humfile:"+humf
            print "Read file :"+humf
            read_sondata(humf,sonD,c1,f1,model1,chunk1)

         print "Correcting : "+humf
            correct(humf,sonD,cww)
            print "Finished Correcting"
```

```
     process(humf,sonD,depth)
        print "Processing for Humfile:"+ humf +" finished."
else:
    print "Unknown input! bye!"
    sys.exit(0)

print "All done. Beer!"
```

APPENDIX C

APPENDIX C

IMAGEJ MACRO

The script will process all images in file directory.

Substitute user defined calibration .txt files for path in line 4.

```
dir = getDirectory("image");
list = getFileList(dir);
for(i=0; i<list.length; i++) {
run("8-bit");
run("Calibrate...",
"open=[C:\\Users\\Student\\Documents\\Mike\\Side_Scan_Data\\Calibration\\Corrected
Calibration\\CorrectedCalibration.txt] function=[Straight Line] unit=[Gray Value]
text1=[187.915 174.4975 161.08 147.6625 134.245 120.8275 107.41 93.9925 80.575 67.1575
53.74 40.3225 26.905 13.4875 0.07 ] text2=[-10.0 -15.0 -20.0 -25.0 -30.0 -35.0 -40.0 -45.0 -
50.0 -55.0 -60.0 -65.0 -70.0 -75.0 -80.0 ] global");
run("Set Scale...", "distance=0 known=0 pixel=1 unit=pixel global");
run("Threshold...");
setThreshold(-55, -10);
run("Analyze Particles...", "size=50-Infinity pixel circularity=0.1-1.00 show=Nothing display
clear summarize");
roiManager("Show All with labels");
roiManager("Show All");
run("Summarize");
name = getTitle;
index = lastIndexOf(name, ".");
if (index!=-1) name = substring(name, 0, index);
name = name + ".xls";
saveAs("Results", dir+name);
run("Open Next");}
```

BIOGRAPHICAL SKETCH

Michael A. Bollinger was born in York, PA and graduated from Dallastown Area High School where he kindled an interest in marine science. His true love for the ocean was instilled by his grandfather, uncle and father on fishing trips in the back bays of Ocean City, MD. His interests led him to study biology and marine science at Penn State University. He quickly became involved in Club Ultimate Frisbee, the Marine Science Society and undergraduate research in the Miksis-Olds' Bioacoustics Lab. He has seized the opportunities to participate in many diving and research experiences all over the world including: The United Kingdom, the Bahamas, Curaçao, Belize, New York, all over the state of Pennsylvania and ultimately led him to Texas.

As a graduate student at the University of Texas Rio Grande Valley, Mike was able to explore the Gulf of Mexico and the field of bioacoustics. At UTRGV he served in several capacities including: mastering the art of soldering and splicing cables together; conducting ongoing diving and fishing surveys of the artificial reefs; helping to maintain research vessels and departmental aquaria; founding the Brownsville Ultimate Frisbee movement; and planning the first two years of the Rio Grande Science and Art Festival. In his spare time, Mike enjoyed long walks on the beach, painting marine life and of course, playing Ultimate Frisbee.

In the future, he hopes to put these acoustic, diving and aquaria skills to use to better manage fish populations. As a final note, remember "many men go fishing all their lives without knowing it is not fish they are after" ~Henry David Thoreau.